SOLAR-PV BASED SINGLE INPUT MULTIPLE OUTPUT (SIMO) DC-DC CONVERTER FOR ELECTRIC VEHICLE APPLICATION

by

NUR IZZATI BINTI ABDUL SAMAD

18018

Dissertation submitted in partial fulfillment of

the requirement for the

Bachelor of Engineering (Hons)

(Electrical and Electronic)

JANUARY 2017

Universiti Teknologi PETRONAS

Bandar Seri Iskandar

31750 Tronoh

Perak Darul Ridzuan

Malaysia

CERTIFICATE OF APPROVAL

SOLAR-PV BASED SINGLE INPUT MULTIPLE OUTPUT (SIMO) DC-DC CONVERTER FOR ELECTRIC VEHICLE APPLICATION

by

Nur Izzati Binti Abdul Samad

18018

A project dissertation submitted to the

Electrical and Electronics Engineering Programme

Universiti Teknologi PETRONAS

in partial fulfillment of the requirement for the

BACHELOR OF ENGINEERING (Hons)

(ELECTRICAL AND ELECTRONICS)

Approved by,

____

(Dr. Ramani Kannan)

UNIVERSITI TEKNOLOGI PETRONAS

BANDAR SERI ISKANDAR, PERAK

JANUARY 2017

CERTIFICATE OF ORIGINALITY

This is to certify that I am responsible for the work submitted in this project, that the original work is my own except as specified in the references and acknowledgement, and that the original work contained herein have not been undertaken or done by unspecified sources or persons.

____

NUR IZZATI BINTI ABDUL SAMAD

ACKNOWLEDGEMENT

First and foremost, I would like to be thankful to Allah for giving me the opportunity to complete my Final Year Project (FYP) for a total of 8 months. Hereby, I would like to express my deep appreciation toward all individuals that involved in assisting me throughout the completion of the project. I also would like to express my special appreciation toward Universiti Teknologi PETRONAS and specifically Electrical and Electronic Engineering Department for providing the opportunity and facilities for the project to be properly conducted.

Besides, I would like to express my special thanks and appreciation towards my project's supervisor and co-supervisor, Dr Ramani Kannnan and Dr Fakhizan Romlie for their continues support as well as their generosity in providing me invaluable wisdom and knowledge related with the project. Their guidance made it possible for me to overcome any obstacles and difficulty faced throughout the project.

My sincere thanks also goes to all my fellow friends for their hard work, continues encouragement and for all the enjoyment that we had within this period. I appreciate all their help and their support.

Lastly, my appreciation goes to my family for their unconditional support and encouragement throughout this project and my life. Their continuous support provided me the courage and strength to face the difficulty during the completion of this project.

ABSTRACT

Electric vehicles and hybrid electric vehicles are seen as the future of the automotive industry with its aim to replace the conventional combustion engine vehicle. This is due to its benefaction in reducing greenhouse gases, the main contributor to rising temperature of the earth. The use of clean and renewable energy efficiently in these vehicles not only helps battling climate change problems that the current generation is facing but also reduces the use of our diminishing natural resources. A DC-DC converter is a type of electric power converter that is used in an electric or hybrid electric vehicle to convert one level of voltage to another for the use of the vehicle's system

The conventional DC-DC circuit used in the electric vehicle is of Multi-Input Multi-Output topology. The drawbacks of this topology are the complexity of circuit which not only increases the size of the converter but also the overall cost. In this research, the novel idea is to implement the Single-Input Multi-Output DC-DC converter topology in an electric vehicle with obtaining input power from solar panel. The circuit modeled was simulated, constructed and evaluated. The proposed idea will be able to overcome the downsides of the conventional method of DC-DC converter used in electric vehicle and thus benefiting users.

TABLE OF CONTENTS

LIST OF FIGURES

LIST OF TABLE

CHAPTER 1:
INTRODUCTION

1.1 Background of Study

Nowadays, the use of electric vehicle and hybrid electric vehicle is seen as a recommended alternative to the conventional combustion engine vehicle. This use of electric vehicle and hybrid electric vehicle contributes in the effort to reduce greenhouse gases which is mainly consisted of CO_2, thus helping in reducing the climate change problems that our generation have been facing in the past few decade. Besides that, the use of clean and renewable energy for these vehicles also lessens the use of our precious natural resources, which is declining at an uncontrollable rate.

The conventional electric and hybrid vehicle uses Multi-Input Multi-Output DC-DC converter topology. This topology is used to get a more reliable and efficient input system. Multiple energy sources such as the fuel cell, solar panel and battery are used. The reason for this multiple installation of renewable energy resources is to make sure that the input energy to the converter is enough. In some circuits, an additional battery is also installed. The reason of installation of battery is that it can be used directionally to provide extra energy when other sources are not available as well as serve as an energy storage component. To date, there has not been a research conducted to test the implementation of SIMO DC-DC converter in an electric vehicle. Thus the possibility and the efficiency of this type of topology installation in a DC-DC converter for the use of electric vehicle are not known.

In this research, the main idea would be to implement the SIMO DC-DC converter in the electric vehicle with the input energy coming from renewable energy resources such as sunlight. The solar panel will be used to provide the energy needed for the system. The input and output of the system will be based on the needs of the electric car and the calculations based on the circuit designed. The limitations of this research would be the implementation of the system in a real electric vehicle. To produce a prototype of this system and its implementation would be costly and impractical. Thus, this research will instead focus on the efficiency of the converter itself as one of the factors affecting the efficiency of the electric vehicle is the efficiency of the converter.

1.2 Problem statements

As stated in the previous section, most of the conventional DC-DC converters in an electric and hybrid are of the Multi Input Multi Output topology. A few drawbacks of the conventional method of the converter have been identified. The drawbacks of the conventional method are as below:

1. Complexity of circuit

   One of the main drawbacks would be the circuit of the conventional Multi Input Multi Output topology is that is has a complex circuit. A complex circuit makes the fabrication and the implementation of the circuit to be difficult.

2. Implementation of multiple switches

   It was also observed that there are multiple switches in the conventional circuit which has multiple inputs. This is to cater the availability of the input renewable energy resources. It is known that having multiple switches in any circuitry increases the switching loss of the system which will be a waste of precious energy.

3. Increase in size and cost of circuit

   The complex circuitry used in the conventional DC-DC converter system not only increases the size and cost of the overall DC-DC converter circuit but also the overall cost of the hybrid vehicle. The cost of the vehicle is an important factor to take note of. As a consumer, one of the main specifications that you look out for in a car would be the cost. The same principle applies for the electric vehicle. An attractive price of an electric vehicle would encourage more people to use the electric vehicle and thus helping in reducing the global greenhouse effect.

Therefore, in this research, an alternative topology is designed to overcome the problems in the conventional topology without neglecting the efficiency and quality of the overall product.

1.3 Objectives

The main objectives of this research would be to

- To study and investigate solar PV model for SIMO converter

- To design a converter circuit to boost operations of electric vehicle application

- To simulate the circuit and analyse the functional output, justifying the results verified through working model

1.4 Scope of study

Based on the objectives stated above, the scope of study for this research would be to design a SIMO converter circuit for the use of electric vehicle. The circuit will be simulated in Multism. The overall circuit will be tested for its efficiency, cost, size and complexity.

After taking into consideration all the data gathered from the test, a decision will be made to verify if the proposed circuit is suitable to be implemented.

CHAPTER 2:
LITERATURE REVIEWS

2.1 Electric and Hybrid Vehicle Technology

One of the most concerning issues in today's world would be the issue of global warming and its effect on our lives and our planet. The matters related to reducing the effects of global warming are taken seriously throughout the globe and this does not exclude the automotive industry [2], [3].

In response to contributing efforts in reducing greenhouse gases, the automobile industry has come up with the Electric Vehicle (EV) and the Hybrid Electric Vehicle (HEV) as an alternative to the conventional combustion engine vehicle [2]. Another reason for choosing an alternative to the conventional method is because of the depletion of our natural resources. By engaging in the EV and HEV technology, the automotive industry is helping in providing a sustainable energy solution that can help preserve our natural resources for the use of future generation. The use of renewable energy resources such as solar energy and environmental friendly fuel cell not only makes the modes of transportation more environmental friendly but also improves fuel efficiency [1]-[4].

Figure 1: The competition between Fossil Fuel and Electric Vehicle

Basically, an EV is a vehicle that replaces the internal combustion engine as well as the transmission systems with an electric one as discussed in [5]. The conventional energy source of the EV would be the rechargeable chemical batteries. But due to the downside of the batteries, such as Ni-Cd (Nickel-Cadminium), Lead Acid, Ni-MH (Nickel Metal Hydride), which are heavy and expensive, more advanced batteries such as the Li-Polymer (Lithium Polymer) and Li-ion (Lithium ion) have gained popularity. Although the advanced batteries are popular, the lead acid type of batteries remains the most practical use in the EV. The topology of basic EV can be seen in Figure 2. The EV has already contributed to the advancement of both the electric drive and storage technology in the HEV as well as the Fuel Cell Vehicle but has been cut back by the automotive industry who declared the HV and the FCV to be the future technology of vehicle.

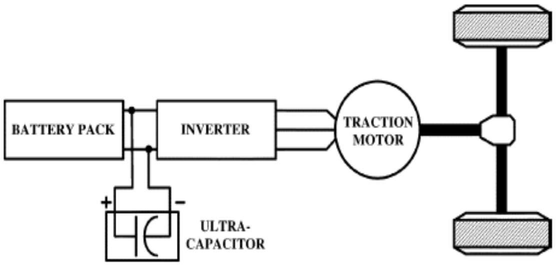

Figure 2: Topology of drive train of EV.

Meanwhile, as stated in [2], the vehicles that use two sources of energy and/or power are called HV. The use of these power and energy sources depends on the vehicle configuration itself. The HEV, by combining the internal combustion engine and the electric motor, minimizes pollution and saves energy. The HEV and be classified by their topologies which are series, parallel and series-parallel [2]-[3], [5].

In a series hybrid vehicle, the source of power for charging batteries is onboard [5] and it is called as such because power flows to the wheels in series [3]. In this configuration, the size of batteries get reduced but in exchange the size of both the generator and engine increase. Among the advantages of the series configuration is that it has low few consumption and high efficiency due to the fact that the vehicle runs on an optional combustion speed and torque. Figure 3 and 4 shows the series HEV propulsion system and the HEV drive train respectively.

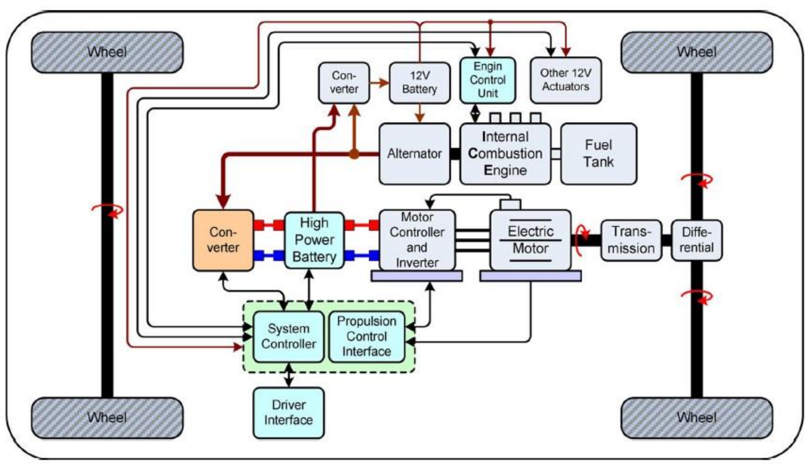

Figure 3: Configuration of series HEV propulsion system.

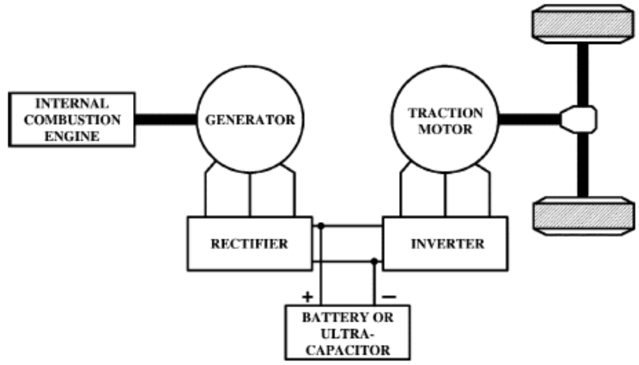

Figure 4: Topology of series HEV drive train.

A parallel HEV is a vehicle that has both the internal combustion engine and the traction motor connected to the transmission in parallel connection [5]. In this type of configuration the engine and the electric motor can be used either separately or together to propel the vehicle. This configuration also has lower fuel consumption due to efficient fuel usage. Some of the advantages of the parallel HEV is that it comes at a lower cost and saves energy while the complexity of the control system becomes the disadvantage. Figure 5 and 6 shows the parallel HEV propulsion system and HEV parallel drive train respectively.

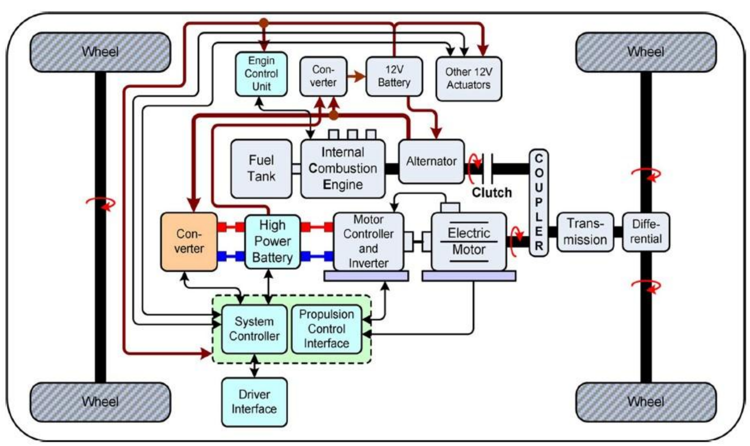

Figure 5: Configuration of parallel HEV propulsion system.

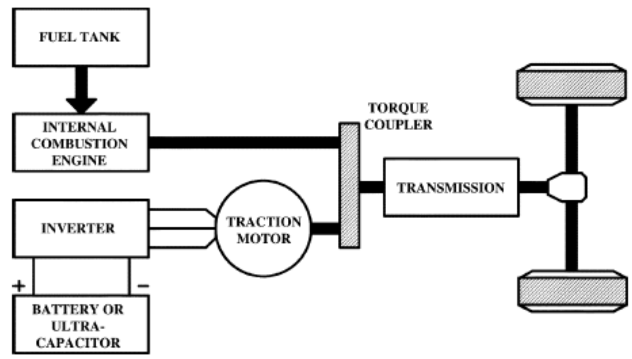

Figure 6: Topology of parallel HEV drive train.

The last configuration would be the series-parallel HEV configuration which is the combination of both of the previous configurations which is done to get the maximum benefit of both types of systems [3], [5]. The downside of this configuration would be that the HEV would be manufactured at a higher cost and more complicated system. Figure 7 displays the drive train for this type of system.

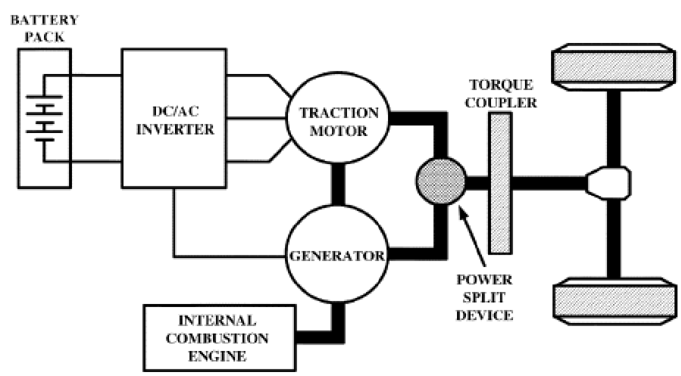

Figure 7: Topology of series-Parallel HEV drive train.

2.2 Types of DC-DC Converters

A DC-DC converter can be considered as a type of electric power converter where one level of voltage is converted to another. This power levels can range anywhere between very low such as in small batteries or very high such as in high-voltage power transmission [6]. A DC-DC converter can be classified as isolated or non-isolated whereby an isolated converter comes with a transformer while non-isolated ones do not. The converters main goal is to reduce both the cost and the number of power components while increasing efficiency and reliability of the system at the same time [7].

The topologies of both the isolated and non-isolated DC-DC converters [8] can be seen in Table 1 below:

Table 1: Isolated and Non-Isolated converter topologies

Isolated DC-DC Converter Topology	Non-Isolated DC-DC Converter Topology
Flyback Forward Push-pull Half-bridge Full-bridge	Buck Boost Buck-boost Cuk SEPIC Zeta CSC

An example of a Full Bridge Topology can be seen in Figure 8 [9] while a SEPIC converter is shown in Figure 9 [8].

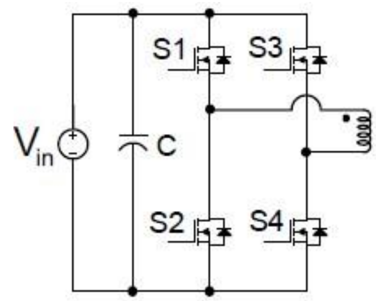

Figure 8: Full-Bridge topology. From [9].

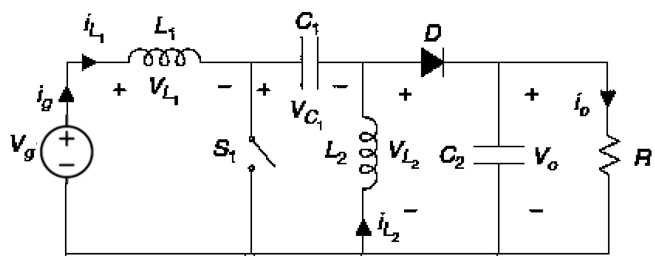

Figure 9: SEPIC converter topology. From [8]

2.3 Non-Isolated DC-DC Converter Topology

As mentioned in the previous section, DC-DC converters can be classified to isolated and non-isolated. In this project, the converter will be of non-isolated type. The configurations of the types of non-isolated DC-DC converters are shown in the figures below[8].

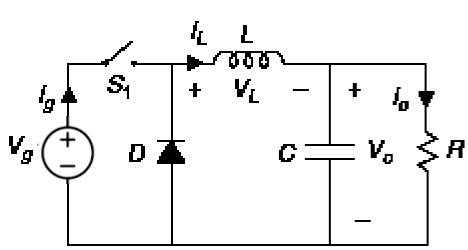

Figure 10: Buck converter topology.

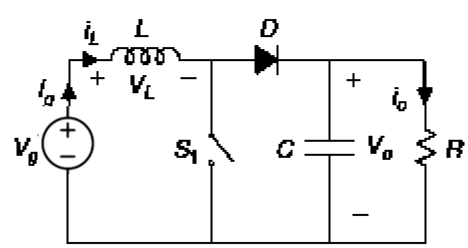

Figure 11: Boost converter topology.

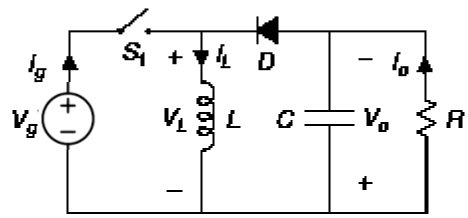

Figure 12: Buck-Boost converter topology.

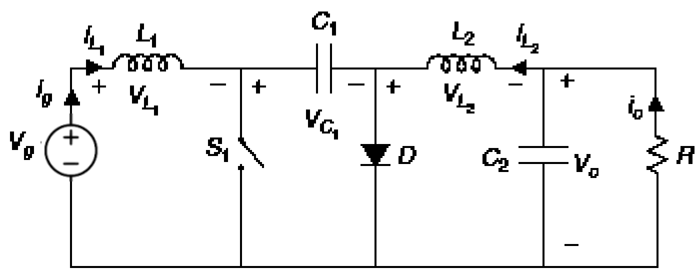

Figure 13: Cuk converter topology.

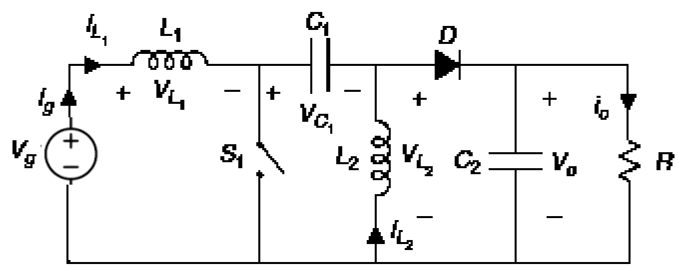

Figure 14: SEPIC converter topology.

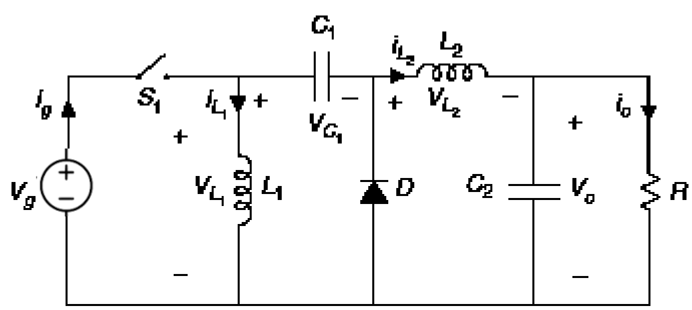

Figure 15: Zeta converter topology.

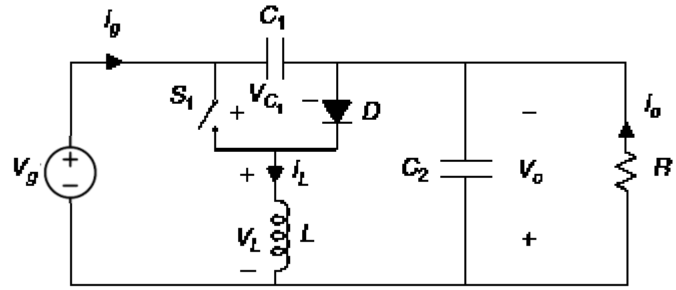

Figure 16: CSC converter topology.

2.4 Non-isolated DC-DC Converter Configuration

The size of a non-isolated DC-DC converter depends on number of active switches employed [8]. This type of converter can be further divided to Single Input Single Output (SISO), Single Input Multiple Output (SIMO), Multiple Input Single Output (MISO) and Multiple Input Multiple Output (MIMO) [7].

Examples of all the topologies stated above can be observed in figures below.

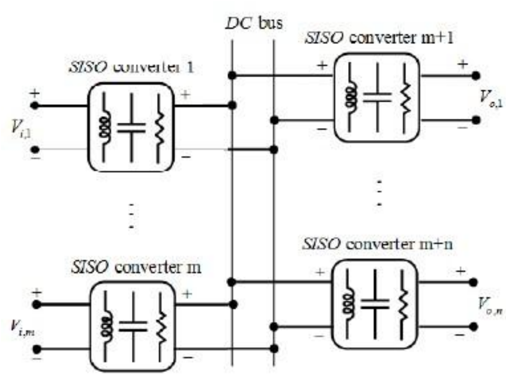

Figure 10: SISO converter topology. From[7]

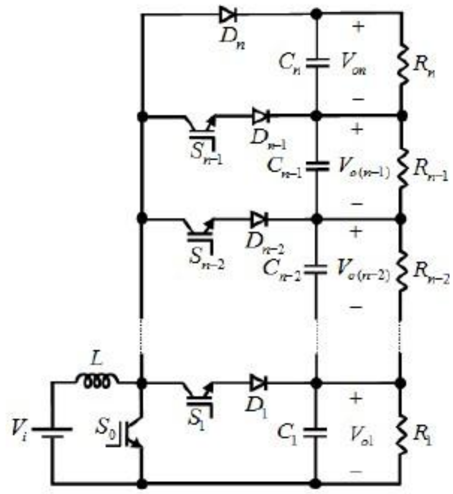

Figure 11: MISO converter topology. From [7]

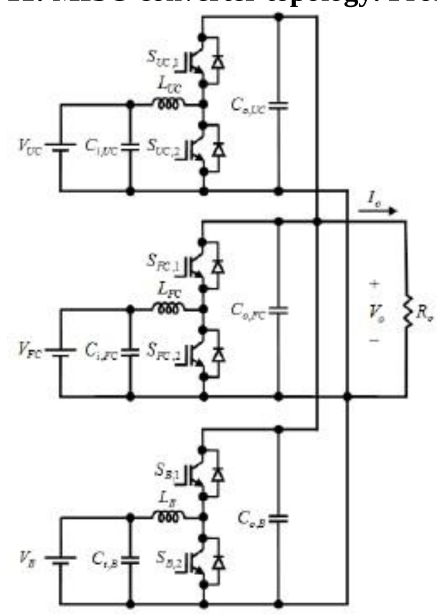

Figure 12: SIMO converter topology. From [7].

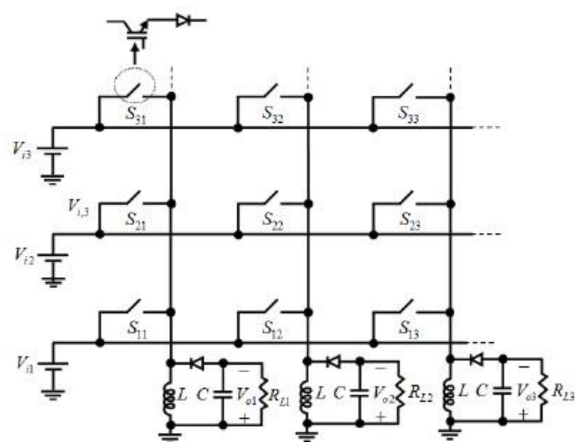

Figure 13: MIMO converter topology. From [7]

2.5 Boost Converter

For this research, the boost converter topology was used as a boost converter acts as a step up converter, which is suitable for this project. It also gives a non-inverted output.

Some of the advantages of boost converter is that it has a simple configuration, high efficiency and has continuous input current [8] that it crucial characteristics to meet and filter electromagnetic interference requirements easily. It also operates at a lower duty cycles and exert low voltage on the MOSFET used as well as give an output voltage that has a lower distortion.

Some of the applications of boost converter can be seen in the figure below:

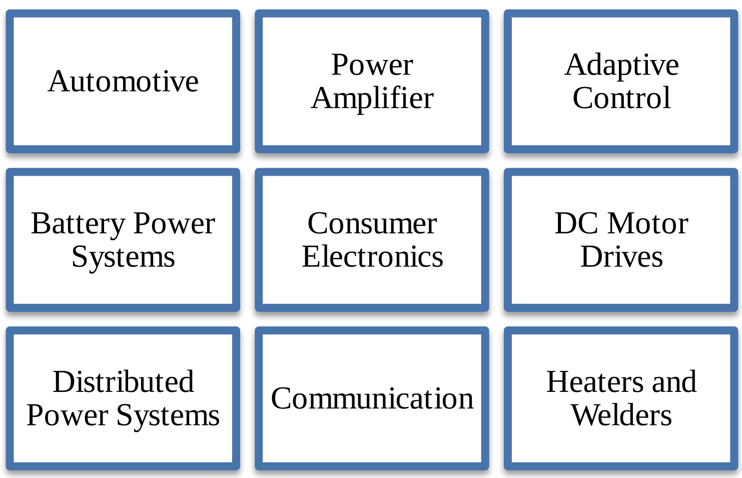

Figure 17: Boost converter application.

2.6 SIMO Configuration

In recent years, SIMO type of configuration of both isolated and non-isolated DC-DC converters received much attention especially in photovoltaic based systems [7]. This is because the SIMO configuration is simple but has high reliability besides being low costing.

This type of configuration is also used because of the limitations of the use of high voltage elements in applications which require high voltages in conventional DC-DC converters. The characteristics of SIMO is that it has a high voltage gain, soft switching and continuous input current and it has been traditionally used in both isolated and non-isolated form.

The applications of SIMO can be seen in the figure below:

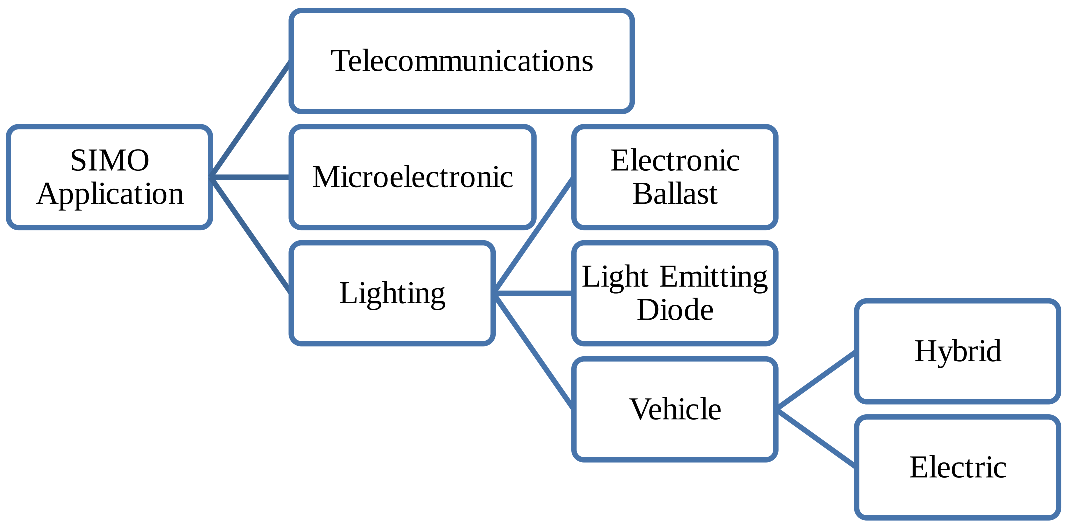

Figure 17: SIMO application.

CHAPTER 3:
METHODOLOGY

3.1 Project Methodology

For this project, since there is a limitation in terms of cost for real life implementation. All the testing was done through computer simulation and the final design of the simulation circuit was then constructed. Based on the data gathered thru the simulations and experimental setup, proper justification was made as a conclusion for this project.

3.1.1 Research Methodology

The research part of this project was done in finding suitable research and experimentation papers online. All the research papers are mainly obtained from approved and valid websites such as the IEEE Explore. Among the subject researched for this project was related to the Electric and Hybrid Vehicle, DC-DC converter topologies, the advantage and disadvantage of DC-DC topologies and implementation of DC-DC converters in electric vehicle. Research was also done for the circuit designing and improvement. The outcome of each paper was observed to find the matters which are related to this project.

3.1.2 LTSpice Simulation

In this project, the design circuit was simulated in the LTSpice software. The values related to the circuit design were based on the calculations on the values of the components from the circuit modeling process. Once the output of the simulation was available, it was analyzed intensively.

The output would have to fulfill certain conditions to be accepted. When the output does not fulfill the conditions, modification was done on necessary parts of the circuit design and value of components was analyzed again for the improvement of the overall converter.

The process was repeated until a desired output was obtained. The final output was analyzed again for the purpose of construction and implementation of the circuit.

3.1.3 Overall Testing and Evaluation

The finalized circuit design based on the simulation was implemented. Tests were done on the overall circuit and the results obtained analyzed. Evaluation of the circuit was also done to justify if it fulfills the conditions set.

The circuit was then tested again, this time based on real working model. As mentioned before, it would be difficult to test the circuit in a real electric car due to the cost limitations. Instead, the circuit was tested with simple components that can be found in an electric car such as light bulb and motors.

Based on all the evaluations of the results obtained, it was observed if the working model of the project manages to solve the problem of the conventional circuit as well as achieved the objectives of the project.

3.1.4 Documentation and Report

Proper documentation is always important in conduction a research. Documentation was be done in each process of this project. This started from the planning phase of the project until the evaluation process. Besides that, the outcome of each of the simulation was recorded for the report of this project. The documentation of this process will help in justifying the results gathered. All of the documentation will then be used to decide if the project has achieved its objectives.

3.2 Project Process Flow

The project process flow for this project is as below

Planning

- Research based on requirements of the project
- Development of Gantt Chart that is feasible and project process flow

↓

Design

- Study of conventional MIMO circuit and finding its flaws in terms of complexity, size and cost
- Determining the design parameters of the circuit based on boost converter configuration

↓

Simulation and Implementation

- Simulation of SIMO converter circuit and constructing the designed circuit for further analysis

↓

Experimentation

Experimentation of the constructed circuit and gathering necessary data for comparison and evaluation purposes.

↓

Comparison

- Analysis and comparison of both the simulation and constructed circuit.
- Justification of results

↓

Documentation and Report

- Proper documentation for the project

3.3 Project Activities

3.3.1 Converter Block Diagram

The figure below shows the basic block diagram of the overall converter. In the figure below the expected input and output values are shown. The input of the converter is from a solar panel rated at 12 V. The solar panel acts as the input of the converter which was designed in this project.

The converter was expected to give multiple outputs at 12V, 24V and 36V. These values were chosen based on the voltage needed for the parts of the system in the EV such as automotive electrical equipment, power steering, air conditioning system and electric motors. These values were taken as the set point values and the performance of the converter was justified based on these input and output values.

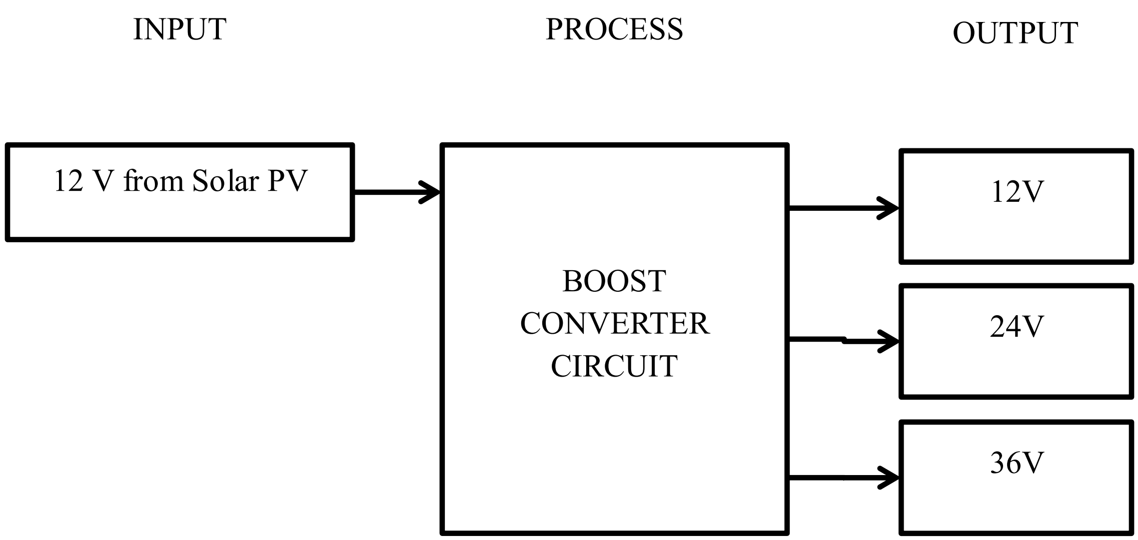

Figure 14: Block Diagram of converter

3.3.2 Solar PV Testing

As mentioned in the previous section, this project used Solar PV as an input source for this converter. The solar photovoltaic or more commonly known as solar cells, convert light energy to electricity in the process called the PV effect. The solar panel rating of 12V was chosen as it is smaller in size and easily acquired.

The voltage output of the solar panel was tested during different hours of the day to get the average value of input voltage. These average values were then used in the simulation and experimental circuit to observe if the designed circuit can give the expected outputs under those conditions. This step was hoped to further justify the reliability aspect of the circuit. The values were taken from sunrise till sunset for three consecutive bright days.

Table 2: Solar Panel Output

	Solar Panel Output (V)			Average (V)
Time	Day 1	Day 2	Day 3	
0700				
0800				
0900				
1000				
1100				
1200				
1300				
1400				
1500				
1600				
1700				
1800				
1900				

Table 2 was used to record the data observed from the solar panel.

3.3.3 Design Modelling of Boost Converter

The simple circuit configuration of the boost converter is as shown in the diagram below

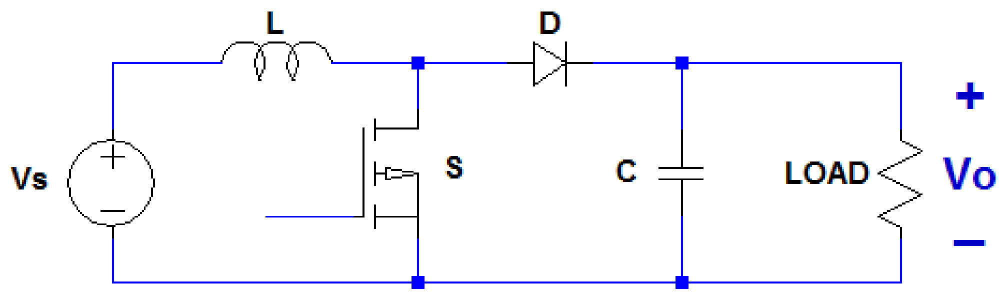

Figure 15: General configuration of boost converter

During CCM operation, the boost converter operation will be as shown below during the ON state of switch, S.

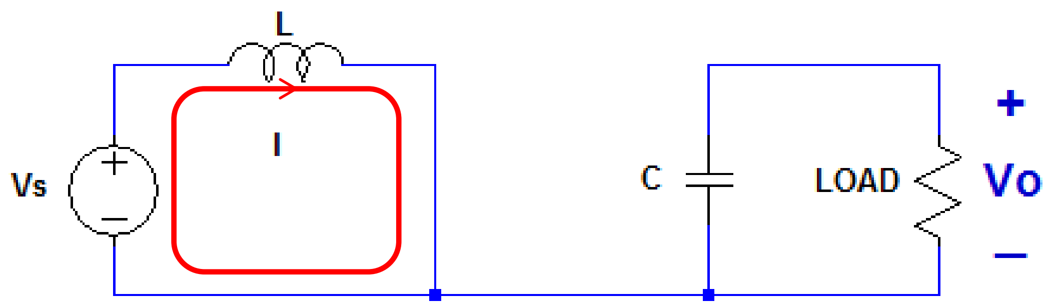

Figure 16: Operation of boost converter during ON state

And during the OFF state of S, the operation is as

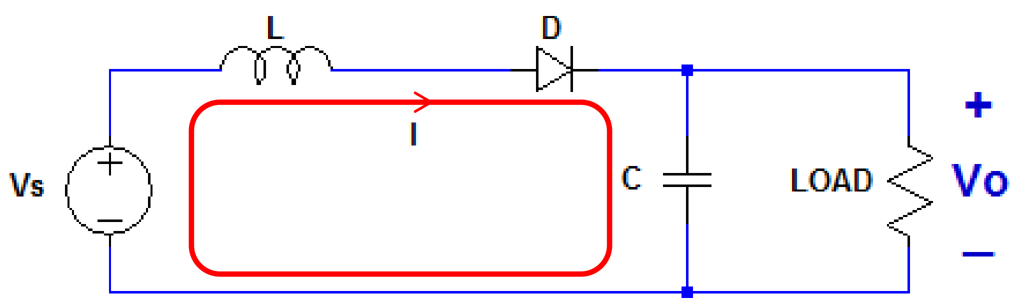

Figure 17: Operation of boost converter during OFF state

In [10] – [12], the equations used in modeling the circuit is discussed. The first step of the calculation of the circuit parameters will be to calculate the duty cycle. The duty cycle of the converter is:

$$D = 1 - \frac{V_{OUT}+V_{FWD}}{V_{IN(min)}+V_{OUT}+V_{FWD}} \tag{1}$$

Where the V_{FWD} in equation (1) is the forward voltage drop of the diode while the input voltage value is taken at a minimum value as this will give the value of maximum switching current. V_{OUT} represents the desired output voltage from the converter. Equation (1) can also be written as shown in equation (2) where the relation between input and output current with duty cycle is shown:

$$\frac{D}{1-D} = \frac{V_{OUT}+V_{FWD}}{V_{IN(min)}+V_{OUT}+V_{FWD}} = \frac{I_{IN}}{I_{OUT}} \tag{2}$$

In selecting the passive components, the inductor ripple current was determined first which is usually set between 20-40% of the input current. This can be observed from the equation:

$$\Delta I_L = 30\%\ X\ \frac{I_{IN}}{\eta} = 30\%\ X\ I_{IN}' \tag{3}$$

The efficiency value, η is usually taken at 80% which is not an unrealistic value for a boost converter. This can be considered as worst case efficiency. In equation 3, the input current is divided by the worst case efficiency and then multiplied by the determined inductor ripple current.

The calculations for the minimum inductor value are as shown in (4):

$$L = \frac{V_{IN(\min)} \times D_{(\max)}}{\Delta I_L \times f_{SW(\min)}} \tag{4}$$

In equation 4, the minimum value of input voltage will be multiplied with the maximum duty cycle and the divided by the product of the calculated inductor ripple current in (3) and the minimum switching frequency.

These calculations are based on the power stage of boost converters which comes with an IC that contains an integrated switch. Thus, it is crucial to know if the selected IC for the converter can deliver the expected maximum value of current. The formula used for this calculation was:

$$I_{OUT(\max)} = (I_{LIM(\min)} - \frac{\Delta I_L}{\eta})\ X\ (1 - D) \tag{5}$$

In the equation, $I_{LIM(min)}$ represents the minimum value of current limit of the IC while the other values such as duty cycle and inductor ripple current values are substituted from the other equations above. The purpose of this is to calculate the maximum output current of the IC and after comparison, determine if the selected IC is suitable for the converter circuit.

The maximum switch current can only calculated if the maximum current output of the IC is above the value of maximum current output of the application. The maximum switch current is as shown below:

$$I_{SW(\max)} = \frac{I_{OUT(\max)}}{1-D} + \frac{\Delta I_L}{2} \tag{6}$$

From the calculations above, the maximum current value that components such as inductor, switches and diode have to be able to withstand.

The next selection of component is the diode, in which it is the rectifier type. In normal conditions, a Schottky diode should be used as it is known to have minimum losses. The value of forward current threshold needs to be same with the maximum current output of the application. Therefore:

$$I_F = I_{OUT(\max)} \tag{7}$$

Where I_F shows the forward current in a rectifying diode. The other calculation based on diode is the power dissipation of the diode which can be calculated by:

$$P_D = I_F \times V_{FWD} \tag{8}$$

This equation, which comprises of forward current and voltage drop across diode can also be written as:

$$P_D = I_{OUT} \times V_{FWD} \tag{9}$$

Usually, the minimum value of input capacitance will be stated in the datasheet of the IC. This value is important to stabilize the input voltage due to peak current requirement of the power supply. The recommended capacitor is that of low equivalent series resistance or better known as ESR ceramic capacitors.

The same principle applies for the output capacitor. The ESR, in this case is used to limit the ripple of the output voltage. The ESR value was calculated as follows:

$$ESR \leq \frac{\Delta V_{RPL}}{(\frac{I_{OUT(\max)}}{1-D_{max}} + \frac{\Delta I_L}{2}} \tag{10}$$

Equation (10) can be rearranged to:

$$\Delta V_{RPL} = ESR \times (\frac{I_{OUT(\max)}}{1-D} + \frac{\Delta I_L}{2}) \tag{11}$$

Where output ripple voltage was calculated. The current flowing through an ESR in a capacitor is one of the causes of power dissipation of a capacitor which leads to the increase of internal temperature of the capacitor. This results in the shortened life of a capacitor. The RMS value of this current ripple is based on:

$$I_{C_{OUT}(RMS)} = I_{OUT} \times \sqrt{\frac{D(\max)}{1-D(\max)}} \tag{12}$$

Meanwhile, the power dissipation in the inductor is also cause by the current flowing through it. Power dissipation is also one of the causes of internal temperature increase of the inductor. This ultimately results in the degradation in the insulation winding, which increases core losses in the inductor. The power loss in the inductor is given by:

$$P_{Inductor} = (\frac{I_{OUT}}{1-D})^2 \times R_{CU} + P_{Core} \tag{13}$$

When selecting the active components, the power MOSFET should be given higher consideration as it should be able to handle the peak voltage and currents besides aiming to minimize the power losses through dissipitation. In this case, the FET's current rating will also determine the boost design converter's maximum output current. The usual type of MOSFET used for boost topology converter is n-channel MOSFET. This is due to the fact that the gate drive is simpler compared to that of p-channel.

The power dissipation of the switch is given by:

$$P_{D\_Q1} = \left[\left(\frac{I_{OUT}}{1-D}\right)^2 \times r_{DS(on)} \times D(\text{max})\right] + \left[\frac{1}{2} \times V_{OUT} \times \left(\frac{I_{OUT}}{1-D}\right)^2 (t_{rise} + t_{fall}) \times f_{SW}\right] + [Q_{GATE} \times V_{GS} \times f_{SW}] \tag{14}$$

3.3.4 Experimental Setup

The simulated circuit was constructed to test the functionality of the converter through a working model. The experimental setup is as shown below in Figure 18. In this setup, the solar panel was substituted with a standard power supply to simplify the data gathering process. An oscilloscope and a multimeter was used to obtain the output values of the converter.

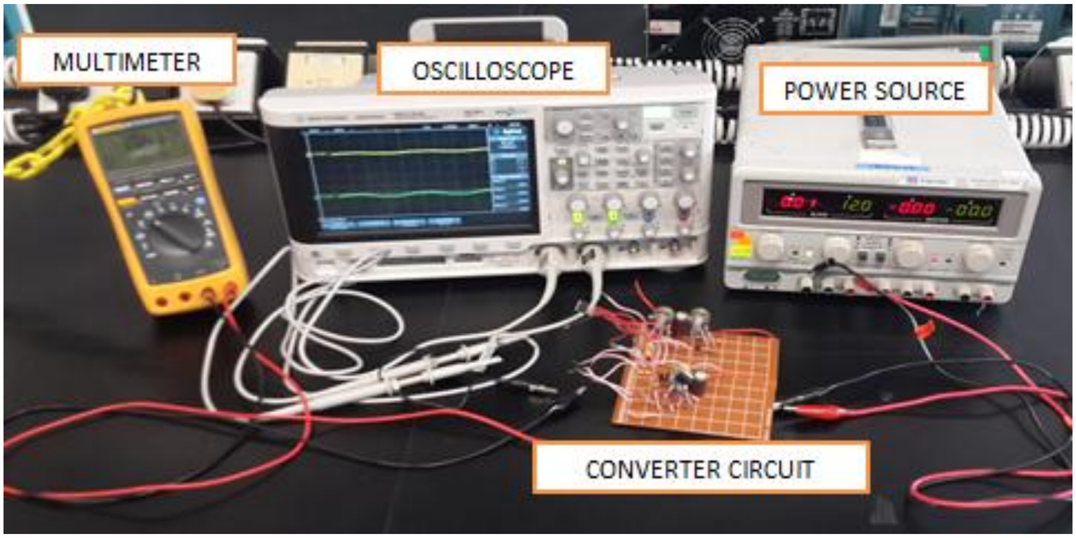

Figure 18: Experimental Setup for testing

The main component in the boost converter is the XL6009 package which is a regulator with fixed frequency PWM. It has the capability to drive a maximum switching current of 5A and a maximum input voltage of 35V.

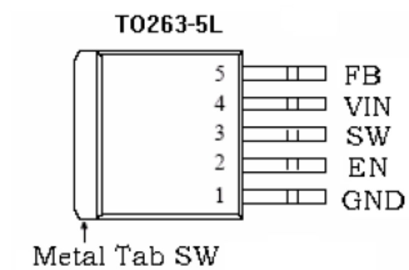

Figure 19: Pin configuration of XL6009 package

The table below lists the description of the pins of the XL6009.

Table 3: Description of XL6009 pins

Pin Number	Pin Name	Description
1	GND	Ground Pin.
2	EN	Enable Pin. Drive EN pin low to turn off the device, drive it high to turn it on. Floating is default high.
3	SW	Power Switch Output Pin (SW).
4	VIN	Input supply voltage pin
5	FB	Feedback pin. Function is to sense the output voltage and regulate it.

The function block diagram of the XL6009 is based on Figure 20.

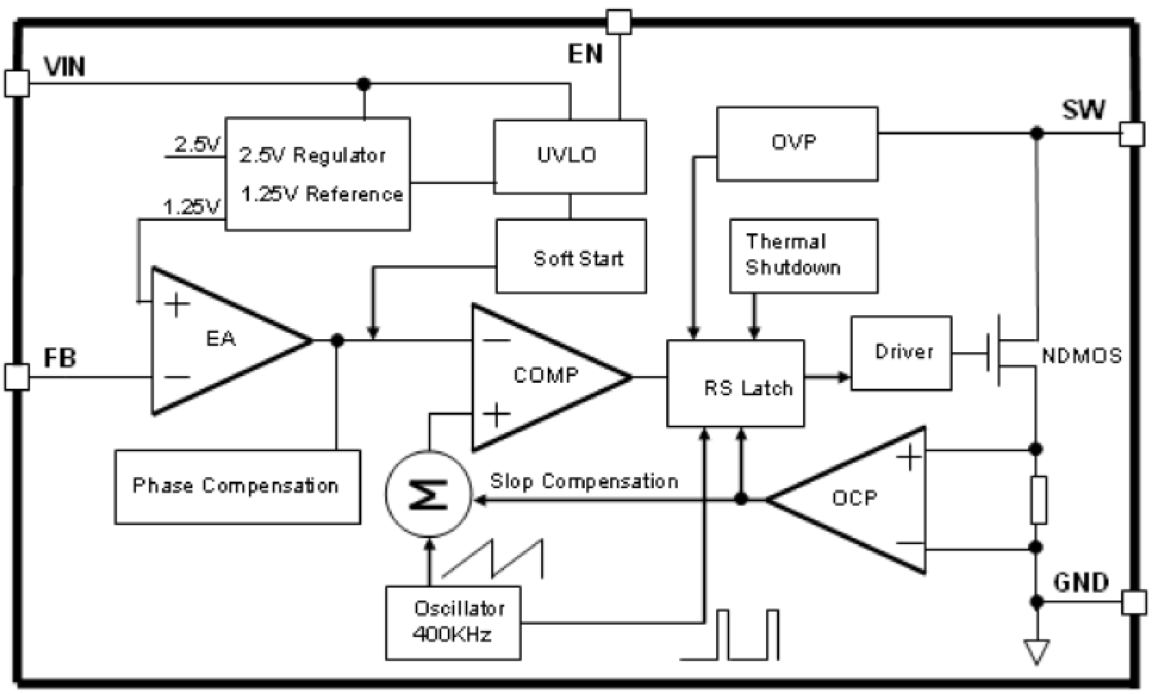

Figure 20: Function block diagram of XL6009

The readings from the oscilloscope and multimeter were tabulated in the form of Table 4 and Table 5. For Table 5, the input voltage was varied from 0V to 12V.

Table 4: Table for Recording Multimeter Readings

Input Voltage (V)	Average Value (V)		
	Output 1 (12V)	Output 2 (24V)	Output 3 (36V)
0			
1			
2			
3			
4			
5			
6			
7			
8			
9			
10			
11			
12			

Table 5: Table for Recording Oscilloscope Readings

Input Voltage (V)	Output Parameters (V)				
	Desired value	Average value	Maximum value	Minimum value	Maximum voltage ripple value
0					
1					
2					
3					
4					
5					
6					
7					
8					
9					
10					
11					
12					
13					
14					
15					

One of the important analyses of the circuit was to calculate the error percentage. This is to find the efficiency of the circuit. The percentage error of the circuit based on the desired and the obtained values can be calculated from the formula below:

$$\%\ error = \left| \frac{Desired\ value - Actual\ value}{Desired\ Value} \right| \times 100\% \quad (16)$$

Based on equation (16), the calculated percentage error was tabulated as below:

Table 6: Calculation of Percentage error

Input Voltage (V)	Desired Value (V)	Actual Value (V)		Percentage error (%)	
		Minimum	Maximum	Minimum	Maximum
0					
1					
2					
3					
4					
5					
6					
7					
8					
9					
10					
11					
12					
13					
14					
15					

3.4 Gantt Chart and Key Milestone

FYP 1 activities	Week Number													
	1	2	3	4	5	6	7	8	9	10	11	12	13	14
Analysis of background of topic and literature review														
Development of block diagram and solution to problem														
Preparation of report for extended proposal														
Designing circuit and calculation of component values														
Submission of extended proposal						√								
Continuation of analysis work for project														
Preparation for proposal defence and report														
Proposal Defence Presentation									√					
Start of simulation work and analysis of the proposed modelling based on the data gathered from the experimentation														
Modification of circuit design and simulation work														
Preparation of Interim Report														
Modelling and design of circuit and cost estimations														
Submission of Interim Draft Report													√	
Submission of Interim Report														√

FYP 2 activities	Week Number														
	1	2	3	4	5	6	7	8	9	10	11	12	13	14	15
Circuit modelling and analysis based on revised converter topology															
Designing circuit and calculation of component values															
Survey of suitable components and purchasing															
Assembly of circuit components based on finalized design of overall circuit															
Analysis of physical circuit to verify simulation results															
Preparation of Progress Report															
Submission of Progress Report								√							
Continuation of analysis and modification of circuit															
Application based testing of circuit															
Preparation for Pre-SEDEX Poster Presentation															
Pre-SEDEX Poster Presentation										√					
Continuation of application based testing and results evaluation															
Finalization of project work															
Preparation of Final Report and Technical Paper															
Submission of Draft Report													√		
Submission of Final Report and Technical Paper														√	
FYP 2 Viva															√

CHAPTER 4:
RESULTS AND DISCUSSION

4.1 Solar PV Output

The solar panel output which was used as the input source to the converter circuit was observed for three consecutive bright days. The setup to take the readings is as in Figure 21.

Figure 21: Setup of Solar Panel

The output voltage from the solar panel on different times of the day was recorded in Table 7.

Table 7: Solar Panel Output Readings

Time	Solar Panel Output (V)			Average (V)
	Day 1	Day 2	Day 3	
0700	7.53	6.80	7.90	7.41
0800	10.70	11.90	12.78	11.79
0900	13.20	13.45	13.20	13.28
1000	14.20	10.60	14.22	13.00
1100	14.20	14.20	12.22	13.54
1200	14.20	14.20	14.22	14.20
1300	14.20	14.20	14.22	14.20
1400	14.22	11.50	14.22	13.31
1500	12.88	12.89	11.50	11.76
1600	10.88	12.89	13.45	12.38
1700	10.50	10.68	12.40	11.19
1800	11.00	10.50	11.78	11.09
1900	7.90	6.90	7.34	7.38

The average value for data above can also be seen in graph below:

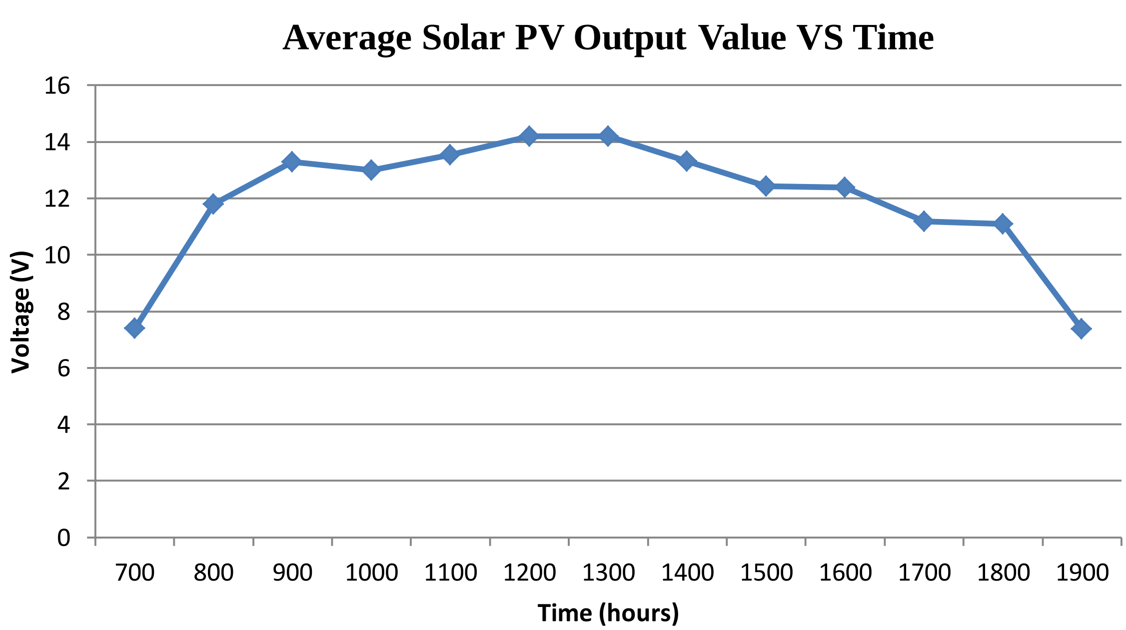

Figure 22: Graph of Average Solar PV Output VS Time

From the results above, it can be seen that the minimum value of solar panel output is 6.9 V while the maximum value is 14.2 V. These values was used during the simulation and testing of circuit to observe if the designed converter can still produce the desired output voltage from the stated input values.

4.2 Simulation of Boost Converter

4.2.1 12 V Output

The simulation of the converter was done part by part based on the output values desired. The first design of the converter was for the 12V output. From the previous section, it was observed that the solar panel output varies with the availability of sunlight. Thus, the first part of the converter was designed in a way that it will always give an output of 12V even if the input voltage varies.

The simulation circuit is as below:

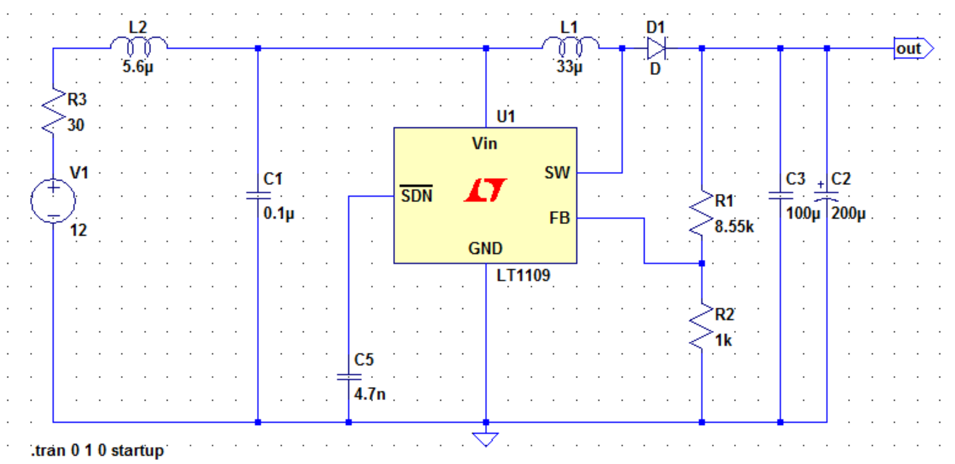

Figure 23: Simulation Circuit for 12V Output

The corresponding waveform is shown below:

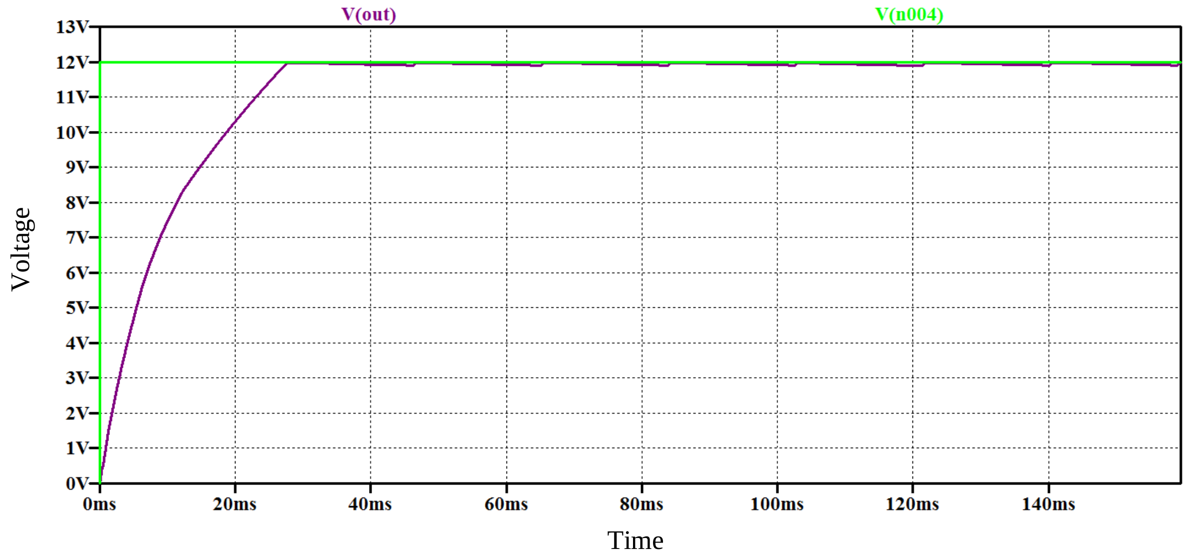

Figure 24: Output Waveform of 12V Circuit

The input voltage was varied and the data from the output waveform is in Table 8:

Table 8: Data from 12V Simulation Output

Input Voltage (V)	Delay Time (s)	Rise Time (s)	Minimum Value (V)	Maximum Value (V)	Voltage Ripple Value (V)
0	0µ	0	0	0	0
1	20.50µ	398m	0.42	0.42	0
2	10.15µ	750.86m	1.50	1.50	0
3	8.38µ	537.52m	11.60	11.60	0
4	7.06µ	271.14m	11.90	11.98	0.08
5	9.05µ	164.82m	11.90	11.98	0.08
6	8.01µ	112.87m	11.90	11.98	0.08
7	6.19µ	82.52m	11.90	11.98	0.08
8	5.38µ	63.20m	11.90	11.98	0.08
9	8.08µ	49.75m	11.89	12.00	0.11
10	5.08µ	40.25m	11.90	11.98	0.08
11	5.24µ	33.09m	11.89	12.00	0.11
12	6.57µ	27.60m	11.90	11.98	0.08
13	3.42µ	24.29m	12.30	12.30	0
14	4.76µ	19.00m	13.28	13.28	0
15	3.55µ	17.00m	14.32	14.32	0

4.2.2 24 V Output

The next part of the converter design was with the output voltage of 24 V. The simulation circuit is as below:

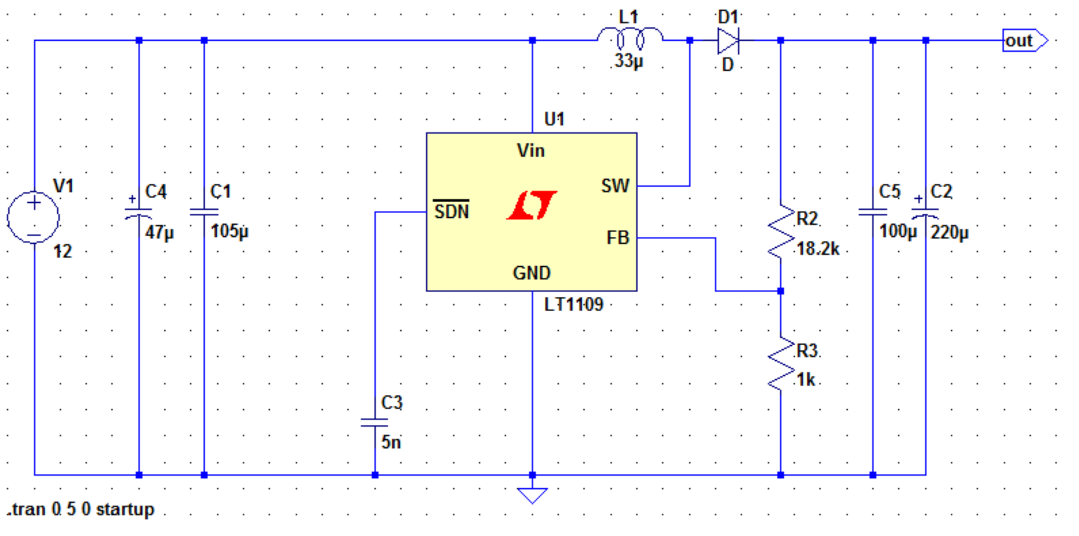

Figure 25: Simulation Circuit for 24V Output

The corresponding graph output is as in Figure 26.

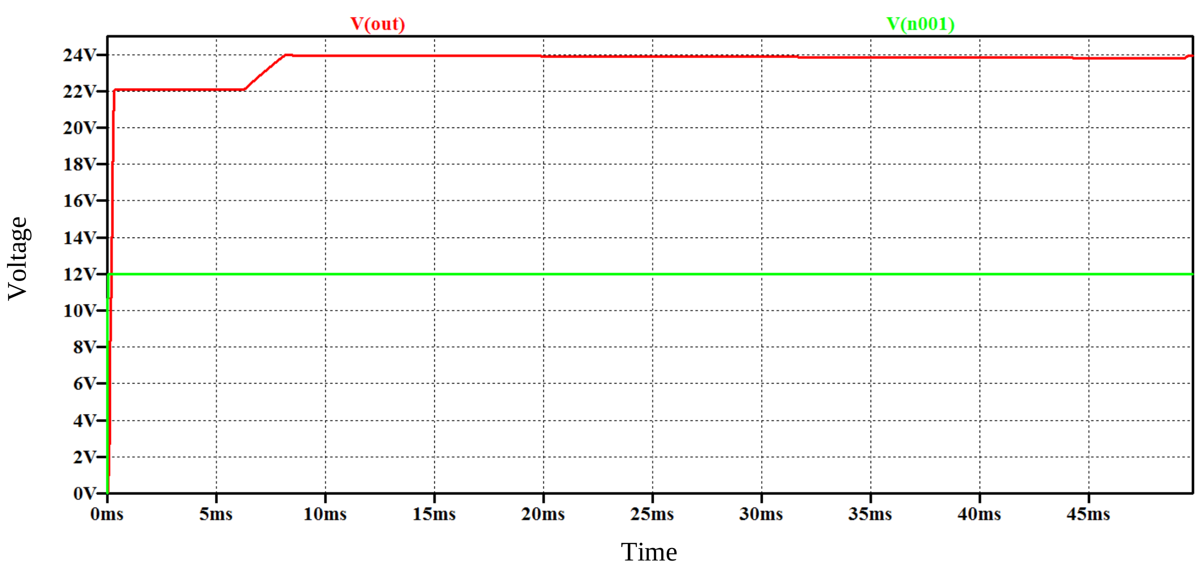

Figure 26: Output Waveform of 24V Circuit

The input voltage was varied and the data from the output waveform is in Table 9:

Table 9: Data from 24V Simulation Output

Input Voltage (V)	Delay Time (s)	Rise Time (s)	Minimum Value (V)	Maximum Value (V)	Voltage Ripple Value (V)
0	0µ	0	0	0	0
1	15.05µ	669.09m	0.44	0.44	0
2	10.69µ	630.05m	14.57	14.63	0.06
3	8.63µ	381.97m	23.76	23.97	0.21
4	6.78µ	190.13m	23.80	23.96	0.16
5	4.05µ	110.16m	23.80	23.97	0.17
6	6.01µ	69.45m	23.80	23.96	0.16
7	5.29µ	46.10m	23.80	23.96	0.16
8	3.78µ	31.85m	23.80	23.97	0.17
9	3.38µ	22.48m	23.80	23.96	0.16
10	2.93µ	15.99m	23.80	23.96	0.16
11	3.31µ	11.49m	23.80	23.97	0.17
12	3.42µ	8.13m	23.80	23.96	0.16
13	6.23µ	6.23m	23.80	23.96	0.16
14	5.05µ	5.59m	23.80	23.97	0.17
15	5.57µ	4.20m	23.80	23.96	0.16

4.2.3 36 V Output

The last part of the converter design was the part with 36 V output. The simulation circuit used was:

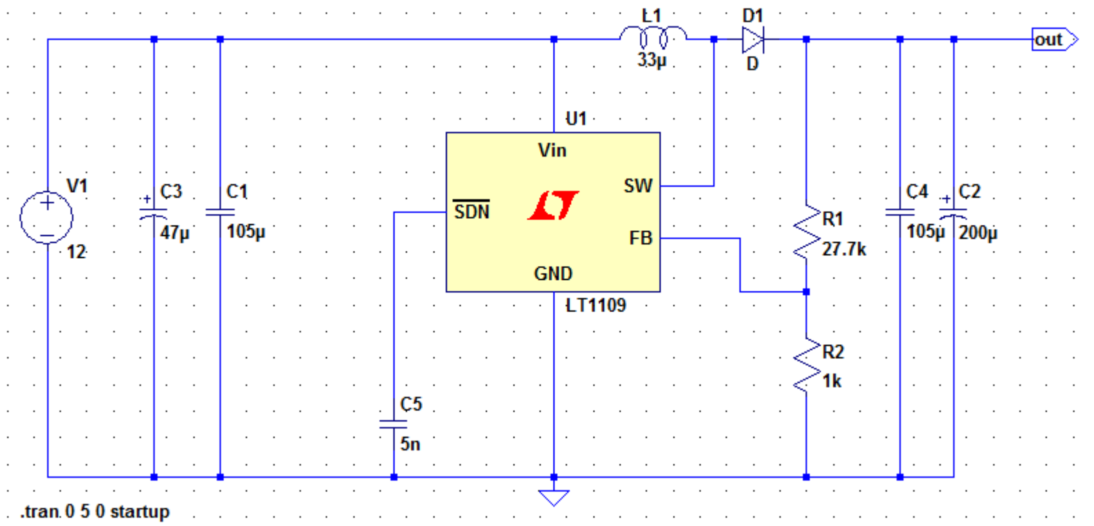

Figure 27: Simulation Circuit for 36V Output

The corresponding waveform is shown in Figure 28. This circuit, similar to those before, was tested under different input source voltage and the data can be seen in Table 10.

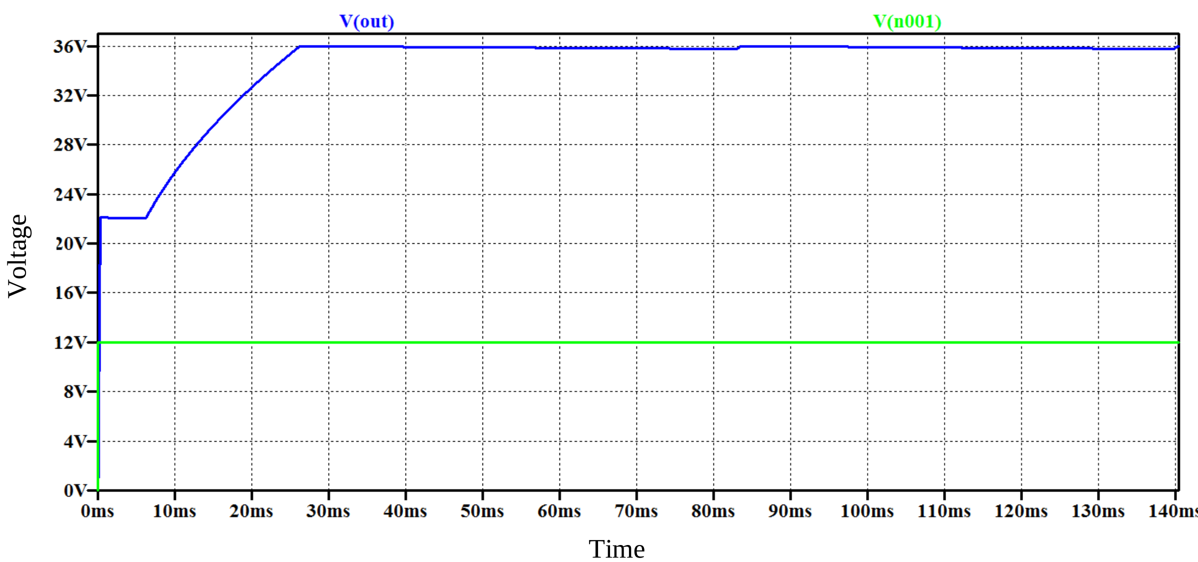

Figure 28: Output Waveform of 36V Circuit

Table 10: Data from 36V Output

Input Voltage (V)	Delay Time (s)	Rise Time (s)	Minimum Value (V)	Maximum Value (V)	Voltage Ripple Value (V)
0	0µ	0m	0.00	0.00	0.00
1	5.34µ	1.34	0.45	0.45	0
2	19.01µ	1.02	12.00	12.45	0.45
3	16.10µ	915.54m	35.75	35.98	0.23
4	9.37µ	448.02m	35.76	35.99	0.23
5	8.29µ	261.99m	35.76	36.00	0.24
6	16.37µ	168.40m	35.76	36.00	0.24
7	8.46µ	114.79m	35.76	35.99	0.23
8	4.37µ	81.88m	35.76	36.00	0.24
9	4.57µ	59.91m	35.76	35.99	0.23
10	5.34µ	44.87m	35.76	35.99	0.23
11	5.24µ	34.19m	35.76	35.99	0.23
12	4.73µ	26.29m	35.76	36.00	0.24
13	5.00µ	20.30m	35.76	35.99	0.23
14	8.09µ	15.72m	35.76	35.99	0.23
15	4.24µ	12.20m	35.76	35.99	0.23

The data gathered was further analysed and the results are as in the graph below which shows the rise time of the output against the input voltage variations.

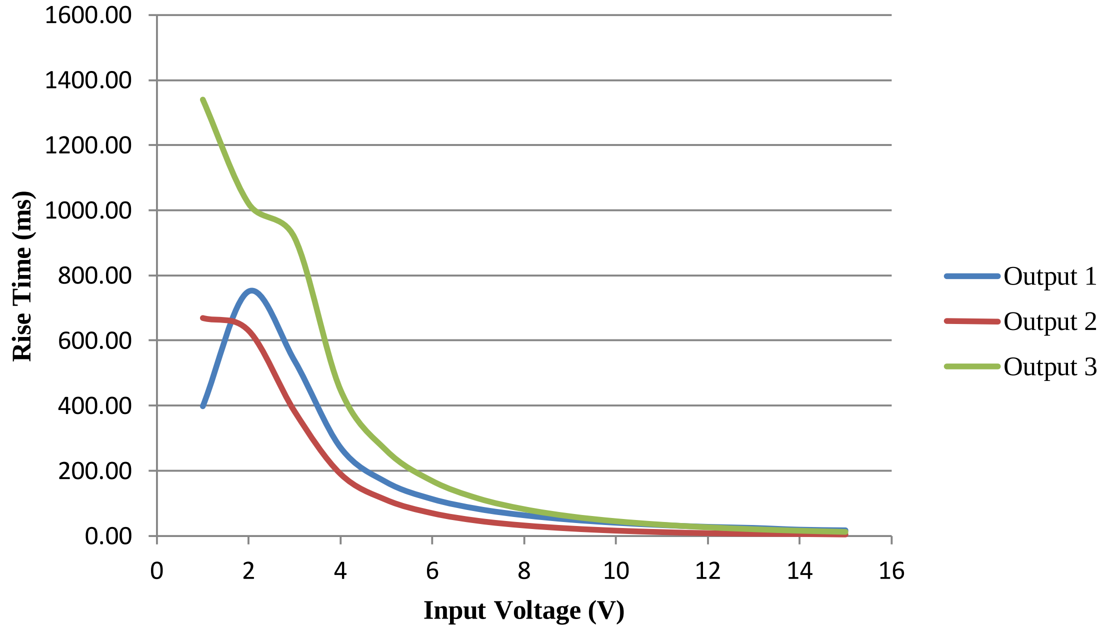

Figure 30: Graph of Input Voltage VS Rise Time

From both the tables and graphs, it can be seen that the output voltage of 24V and 36V are stable with the variation of input voltage from 6V to 15V. In contrast, the 12V output only achives it’s desired output with input voltage of 6V to 12V. When the input voltage is higher than 12V, the output voltage also increases, causing it to have final value error. This resonates with the concept of boost converter whereby the input voltage should be lower than the output voltage. Thus it is crucial that the input voltage of the converter to be maintained at 12V and below. Meanwhile, the second graph indicates that as the input voltage decreaese, the rise time of the converter output increases.

4.2.4 Overall Converter Output

All the three circuit schematics shown above were combined and the resulting circuit is as shown in Figure 31.

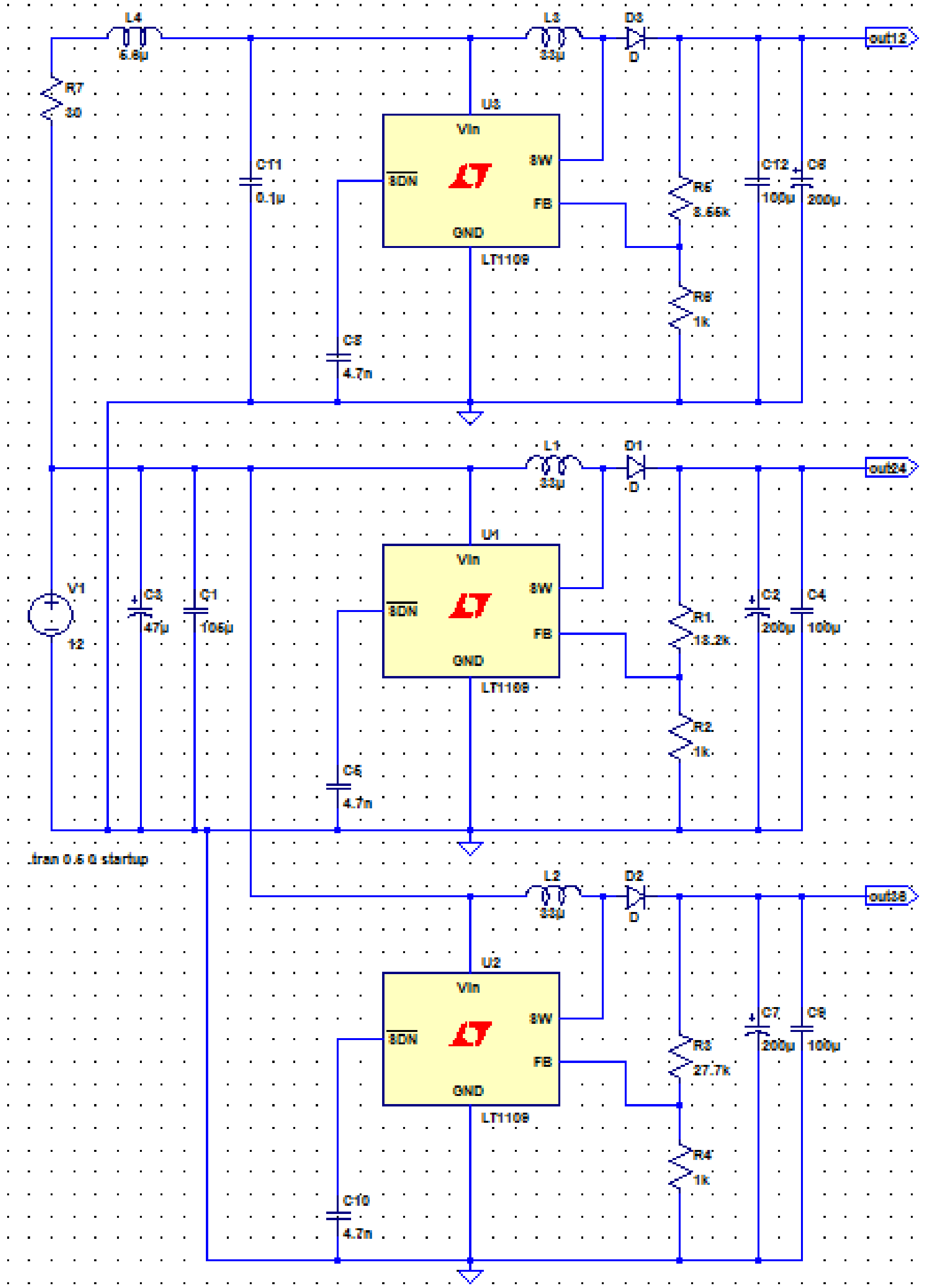

Figure 31: Simulation Circuit of Converter

The corresponding waveform of the circuit is as below. The input voltage is set to 12V which is in green in colour. The purple waveform if of that from the 12V output while the red and blue waveform indicates the 24V and 36V output respectively.

The output of the circuit is as below and it can be seen that all the outputs of the circuit achieves the desired output target.

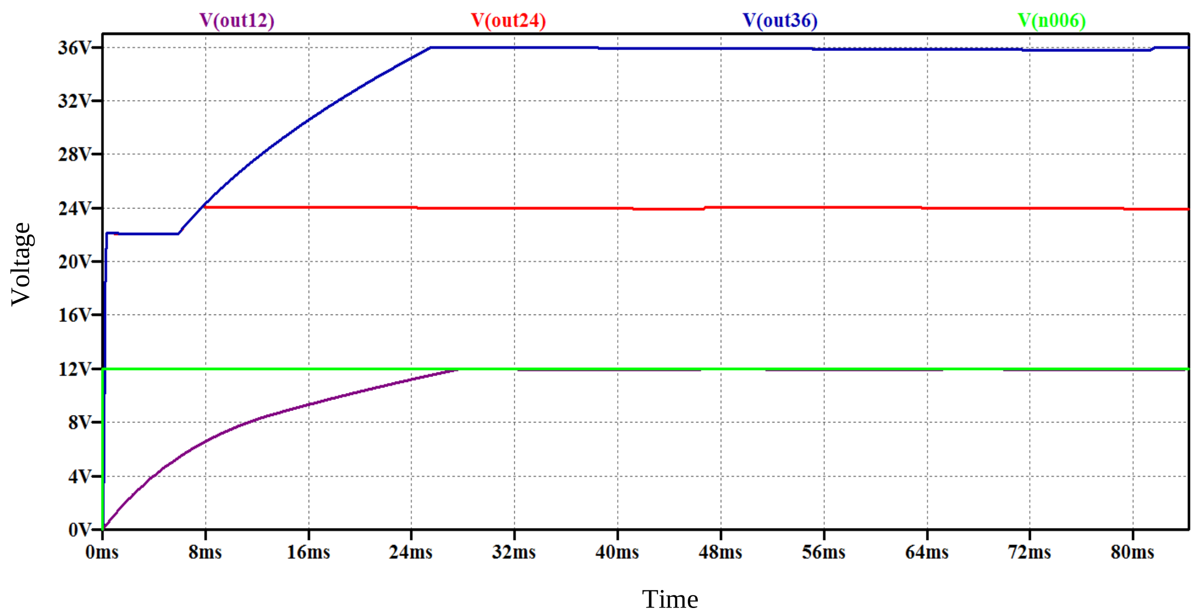

Figure 32: Output Waveform of Converter Circuit

4.3 Experimental Results

The circuit for the converter was constructed based on the overall block diagram. The figure below shows the setup for the testing phase of the circuit. In this testing phase, the 12V solar PV was substituted with a voltage supply to make the testing and gathering of data more convinient. A multimeter and oscilloscope was used to take readings from both the input and the outputs from the circuit. The values observed was gathered and will be used to determine of the circuit fulfills its function and objectives of this project.

Table 11 shows the outputs of the converter when the input voltage is varied from 0V to 12V. The average value was taken from the reading of multimeter.

Table 11: Multimeter Readings

Input Voltage (V)	Average Value (V)		
	Output 1 (12V)	Output 2 (24V)	Output 3 (36V)
0	0	0	0
1	0.4	0.4	0.4
2	1.5	1.7	1.7
3	4.1	22.8	27.0
4	7.6	23.9	35.8
5	11.48	23.9	36.0
6	12.0	23.9	35.8
7	12.0	24.0	35.8
8	12.0	23.9	35.9
9	12.0	23.9	35.9
10	11.9	24.0	35.8
11	12.0	24.0	36.0
12	12.0	24.0	36.0
13	12.1	24.0	36.0
14	13.8	23.9	36.0
15	14.3	24.0	36.0

Further analysis was done using the oscilloscope and the screenshot of the equipment as shown in Figures 34 to 36. Based on the readings of the oscilloscope, the output parameters were recorded in the tables for Output 1, Output 2, and Output 3 respectively.

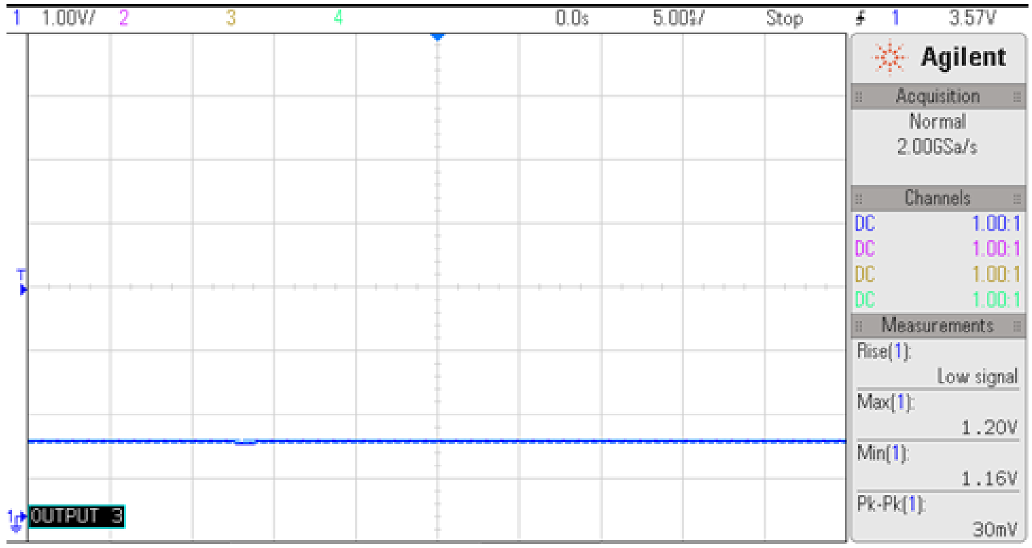

Figure 34: Oscilloscope Output for 12V

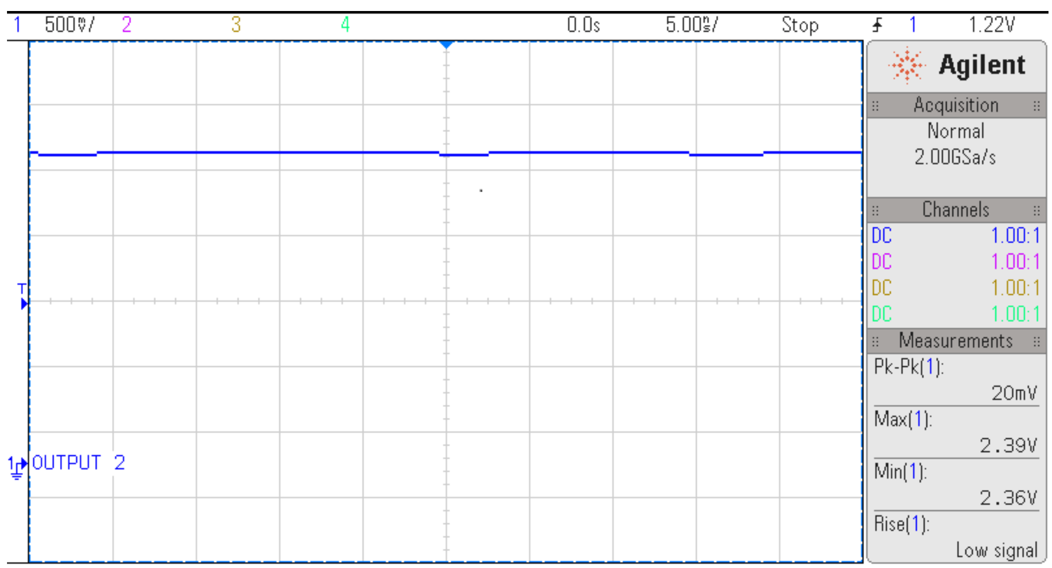

Figure 35: Oscilloscope Output for 24V

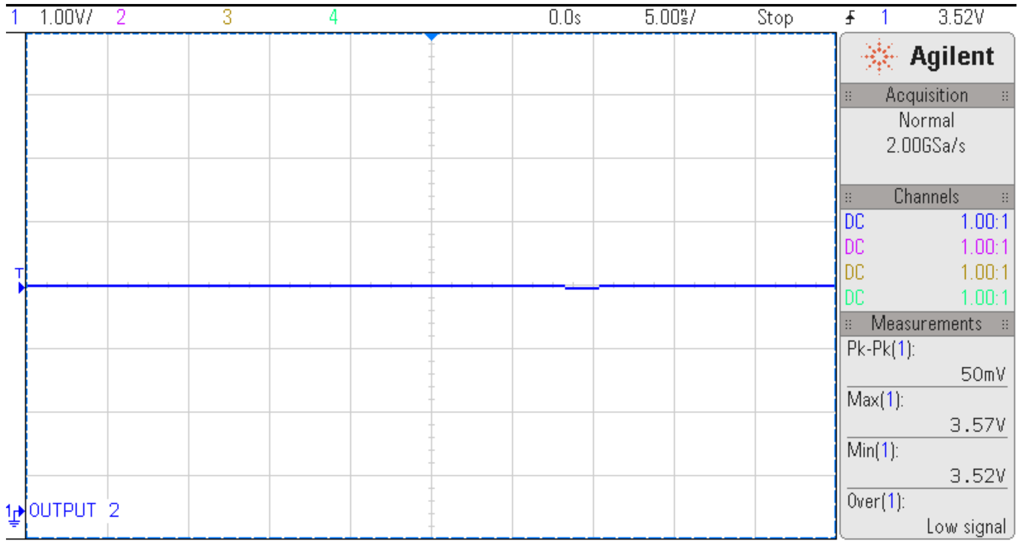

Figure 36: Oscilloscope Output for 36V

Table 12: Oscilloscope Readings Output 1

Input Voltage (V)	Output Parameters (V)			
	Desired value	Maximum value	Minimum value	Maximum voltage ripple value
0.0	12.0	0.0	0.0	0.0
1.0	12.0	0.4	0.0	0.4
2.0	12.0	1.3	0.8	0.5
3.0	12.0	4.1	3.6	0.5
4.0	12.0	7.3	6.9	0.4
5.0	12.0	11.4	11.2	0.2
6.0	12.0	12.0	11.7	0.3
7.0	12.0	12.1	11.7	0.4
8.0	12.0	12.0	11.7	0.3
9.0	12.0	11.9	11.7	0.2
10.0	12.0	12.0	11.7	0.3
11.0	12.0	12.0	11.7	0.3
12.0	12.0	12.0	11.7	0.3
13.0	12.0	12.5	12.1	0.4
14.0	12.0	13.4	12.9	0.5
15.0	12.0	14.3	14.1	0.2

Table 13: Oscilloscope Readings Output 2

Input Voltage (V)	Output Parameters (V)			
	Desired value	Maximum value	Minimum value	Maximum voltage ripple value
0.0	24.0	0.0	0.0	0.0
1.0	24.0	0.4	0.0	0.4
2.0	24.0	1.5	1.0	0.5
3.0	24.0	22.8	22.3	0.5
4.0	24.0	24.0	23.7	0.3
5.0	24.0	24.0	23.5	0.5
6.0	24.0	23.9	23.5	0.4
7.0	24.0	24.0	24.0	0.0
8.0	24.0	24.0	23.5	0.5
9.0	24.0	24.0	23.5	0.5
10.0	24.0	24.0	23.5	0.5
11.0	24.0	24.0	23.5	0.5
12.0	24.0	24.0	23.8	0.2
13.0	24.0	24.1	23.6	0.5
14.0	24.0	24.0	23.5	0.5
15.0	24.0	24.0	23.5	0.5

Table 14: Oscilloscope Readings Output 3

Input Voltage (V)	Output Parameters (V)			
	Desired value	Maximum value	Minimum value	Maximum voltage ripple value
0.0	36.0	0.1	0.0	0.0
1.0	36.0	0.3	0.0	0.3
2.0	36.0	1.5	1.0	0.5
3.0	36.0	26.8	26.3	0.5
4.0	36.0	35.7	35.2	0.5
5.0	36.0	35.9	35.4	0.5
6.0	36.0	35.7	35.2	0.5
7.0	36.0	35.8	35.4	0.4
8.0	36.0	35.9	35.4	0.5
9.0	36.0	35.7	35.2	0.5
10.0	36.0	35.8	35.3	0.5
11.0	36.0	35.8	35.4	0.4
12.0	36.0	35.7	35.2	0.5
13.0	36.0	35.7	35.2	0.5
14.0	36.0	35.7	35.2	0.5
15.0	36.0	35.7	35.2	0.5

Meanwhile, the percentage errors for each of the output based on the variations of input voltage were recorded from the readings of oscilloscope and the data were tabulated as in the tables below:

Table 15: Calculation of Percentage error for Output 1

Input Voltage (V)	Desired Value (V)	Actual Value (V)		Percentage error (%)	
		Minimum	Maximum	Minimum	Maximum
0.0	12.0	0.0	0.0	100.0	100.0
1.0	12.0	0.0	0.4	96.7	100.0
2.0	12.0	0.8	1.3	89.2	93.3
3.0	12.0	3.6	4.1	65.8	70.0
4.0	12.0	6.9	7.3	39.2	42.5
5.0	12.0	11.2	11.4	5.0	6.7
6.0	12.0	11.7	12.0	0.0	2.5
7.0	12.0	11.7	12.1	-0.8	2.5
8.0	12.0	11.7	12.0	0.0	2.5
9.0	12.0	11.7	11.9	0.8	2.5
10.0	12.0	11.7	12.0	0.0	2.5
11.0	12.0	11.7	12.0	0.0	2.5
12.0	12.0	11.7	12.0	0.0	2.5
13.0	12.0	12.1	12.5	0.8	4.2
14.0	12.0	12.9	13.4	7.5	11.7
15.0	12.0	14.1	14.3	17.5	19.2

Table 16: Calculation of Percentage error for Output 2

Input Voltage (V)	Desired Value (V)	Actual Value (V)		Percentage error (%)	
		Minimum	Maximum	Minimum	Maximum
0.0	24.0	0.0	0.0	100.0	100.0
1.0	24.0	0.0	0.4	98.3	100.0
2.0	24.0	1.0	1.5	93.8	95.8
3.0	24.0	22.3	22.8	5.0	7.1
4.0	24.0	23.7	24.0	0.0	1.3
5.0	24.0	23.5	24.0	0.0	2.1
6.0	24.0	23.5	23.9	0.4	2.1
7.0	24.0	24.0	24.0	0.0	0.0
8.0	24.0	23.5	24.0	0.0	2.1
9.0	24.0	23.5	24.0	0.0	2.1
10.0	24.0	23.5	24.0	0.0	2.1
11.0	24.0	23.5	24.0	0.0	2.1
12.0	24.0	23.8	24.0	0.0	0.8
13.0	24.0	23.6	24.1	0.4	1.7
14.0	24.0	23.5	24.0	0.0	2.1
15.0	24.0	23.5	24.0	0.0	2.1

Table 17: Calculation of Percentage error for Output 3

Input Voltage (V)	Desired Value (V)	Actual Value (V)		Percentage error (%)	
		Minimum	Maximum	Minimum	Maximum
0.0	36.0	0.0	0.1	99.7	100.0
1.0	36.0	0.0	0.3	99.2	100.0
2.0	36.0	1.0	1.5	95.8	97.2
3.0	36.0	26.3	26.8	25.6	26.9
4.0	36.0	35.2	35.7	0.8	2.2
5.0	36.0	35.4	35.9	0.3	1.7
6.0	36.0	35.2	35.7	0.8	2.2
7.0	36.0	35.4	35.8	0.6	1.7
8.0	36.0	35.4	35.9	0.3	1.7
9.0	36.0	35.2	35.7	0.8	2.2
10.0	36.0	35.3	35.8	0.6	1.9
11.0	36.0	35.4	35.8	0.6	1.7
12.0	36.0	35.2	35.7	0.8	2.2
13.0	36.0	35.2	35.7	0.8	2.2
14.0	36.0	35.2	35.7	0.8	2.2
15.0	36.0	35.2	35.7	0.8	2.2

4.4 Comparison of Simulation and Experimental Results

From the simulation and experimentation results obtained above, comparisons were done on several aspects. This includes the output voltage based on input voltage variations, stability of output voltages and percentage error. These comparisons were used to see if the constructed circuit has similar results to the simulated one.

4.4.1 Input Voltage Variations

The graph below shows the output voltages when the input voltage was varied based on the simulation results

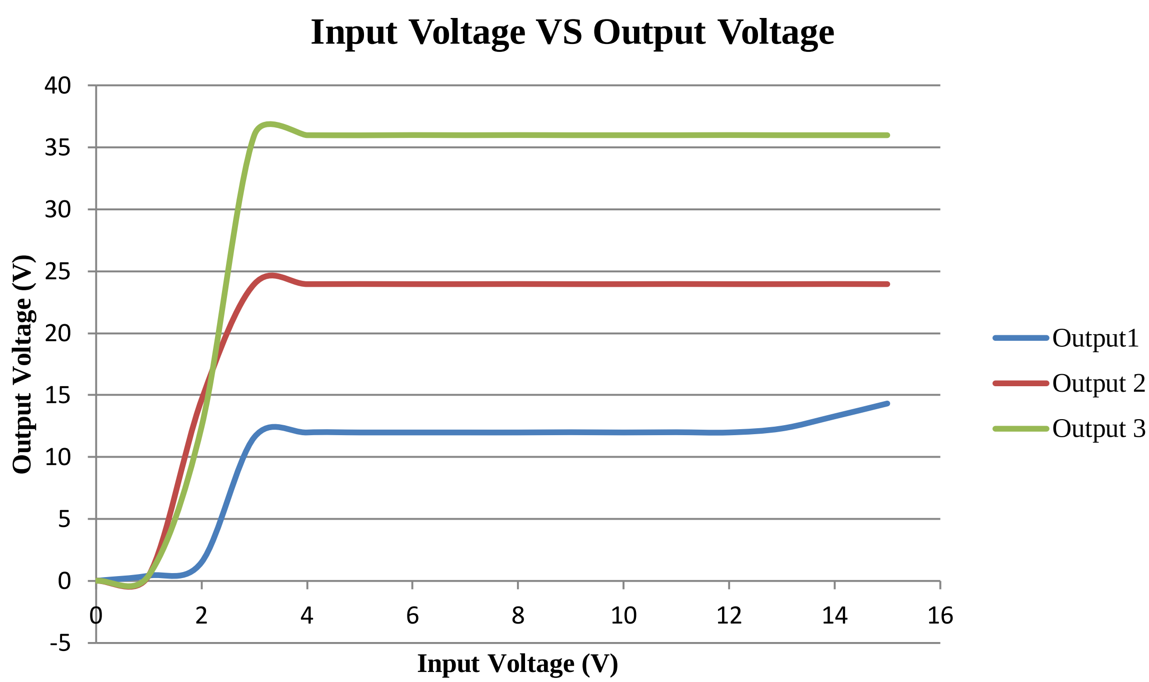

Figure 34: Graph of Input Voltage VS Output Voltage from Simulation results

The graph below shows the voltages when input was varied based on experimental results. The values were the ones obtained from oscilloscope.

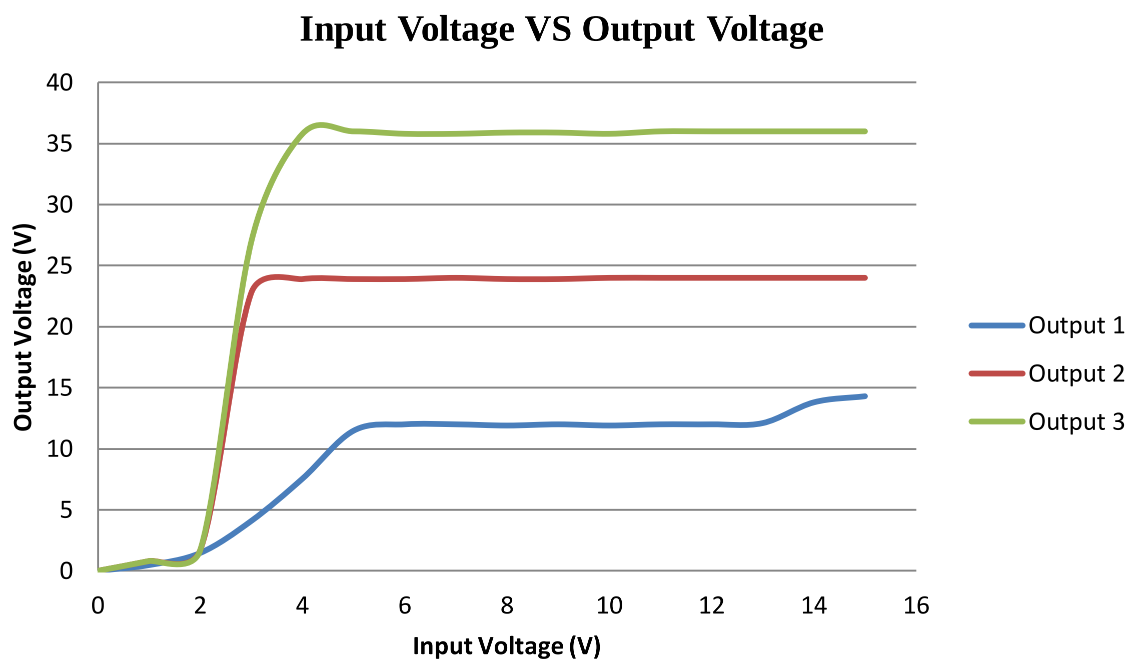

Figure 35: Graph of Input Voltage VS Output Voltage from Experimental results

From both the graphs of simualtion and experimental results, it can be seen that the outputs does have a differenece. In the simulated circuit, all the three outputs were achieved with input of only 3 V whereas in the experimental results, the constructed circuit needs at least 5 V to get all the desired ouput voltages. Both the results are shown to be stable as the input voltage was increased. Finally, it can be seen that both the Output 1 of the circuits which is the 12V output increases after input voltage above 12V is applied. This resonates with the fact that in boost converter topology, the input voltage should be less than the output volatge.

4.4.2 Percentage Error

The graphs below show the maximum percentage error of each of the simulated and constructed converter circuit output.

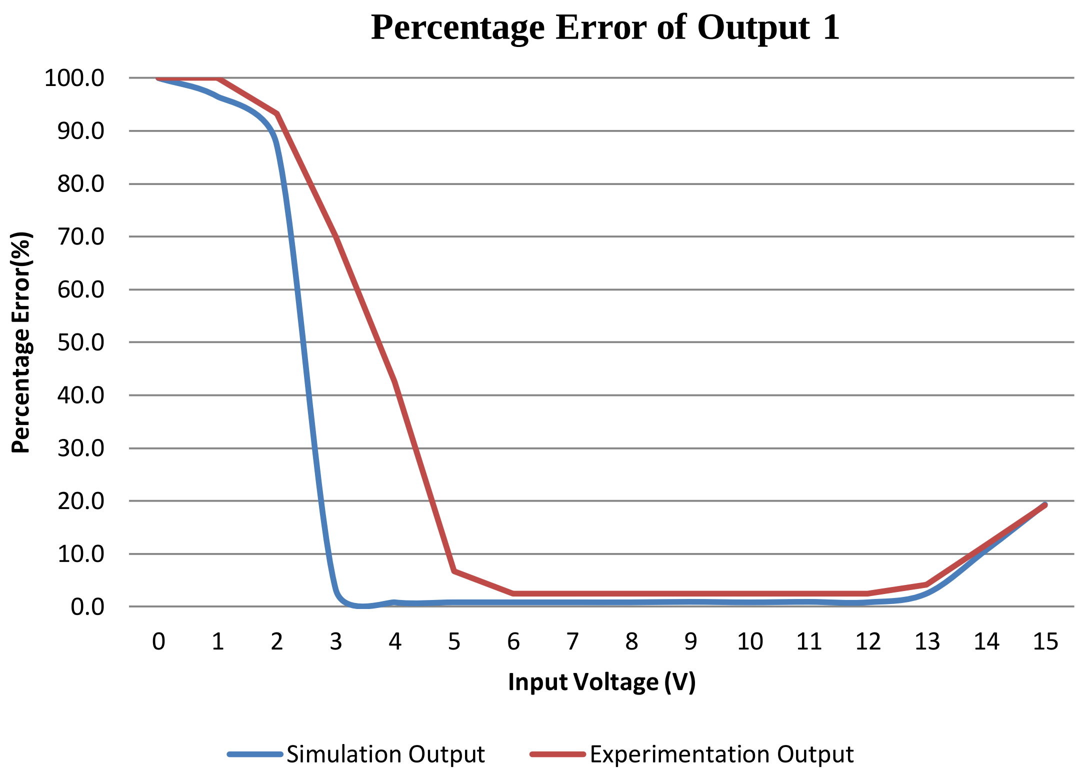

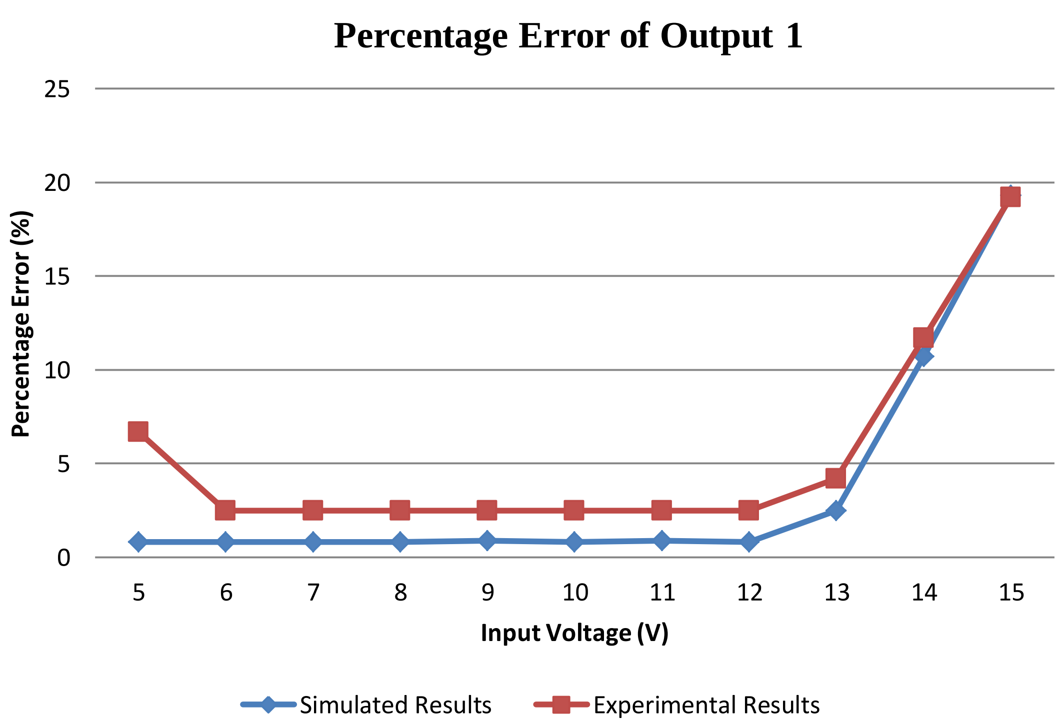

Figure 35: Percentage Error of Output 1

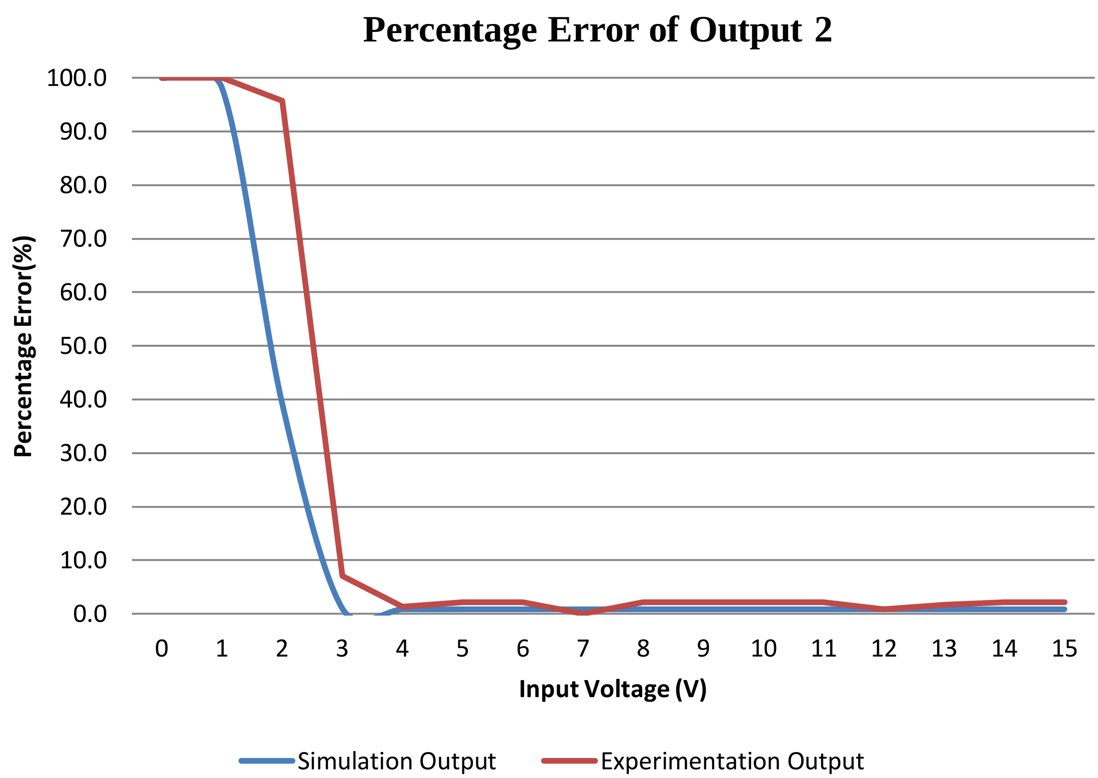

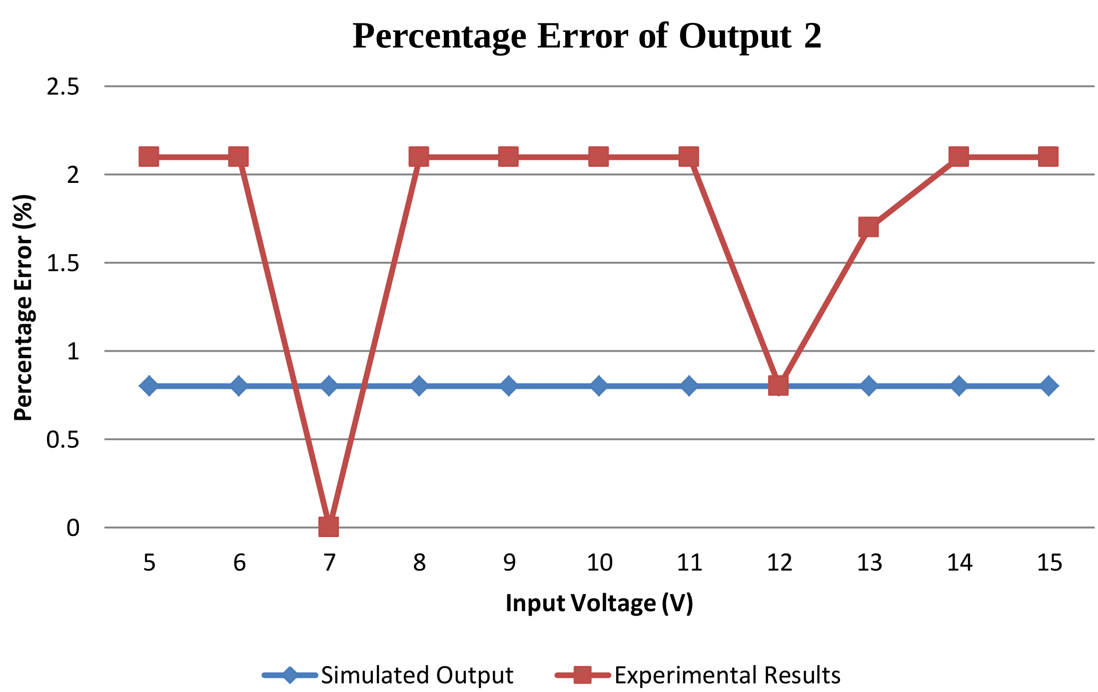

Figure 35: Percentage Error of Output 2

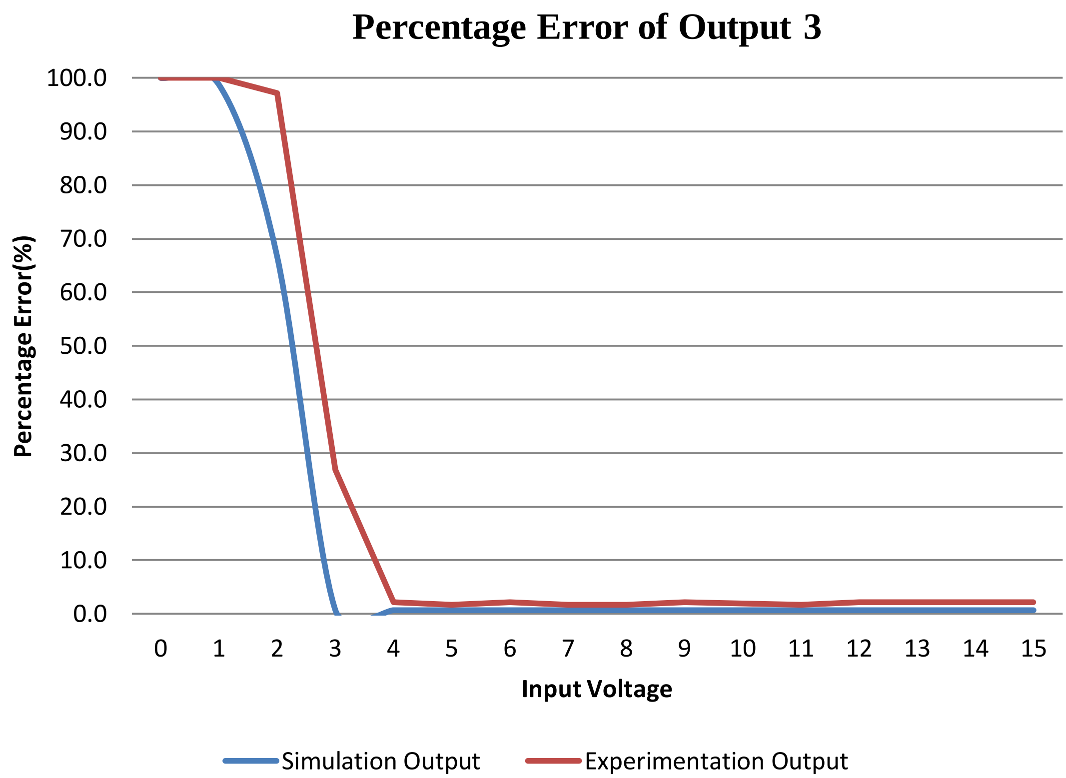

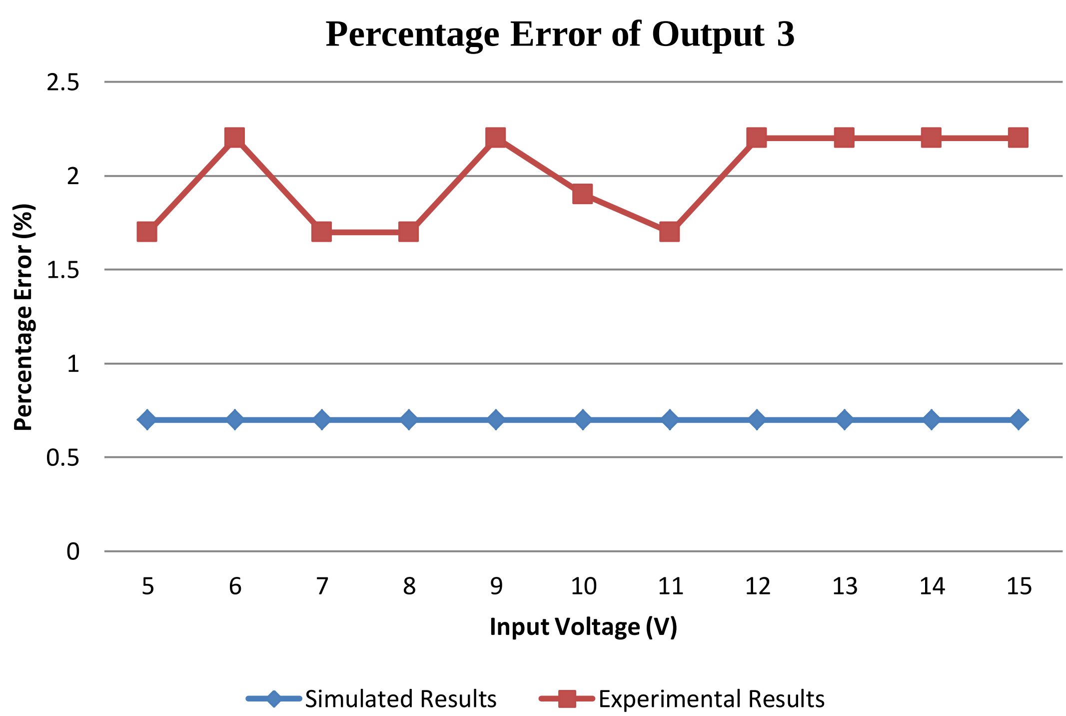

Figure 35: Percentage Error of Output 3

From all the graphs above showing the percentage error, it can be observed that the simulated results and experimental results show some variations. In the simulation, the percentage error is at a stable value while in all three experimentation, the percentage error changes from one point to another. But the overall percentage error of the constructed circuit is below 10% which shows that the converter is reliable and accurate.

CHAPTER 5:
CONCLUSION AND RECOMMENDATION

5.1 Conclusion

As a conclusion, the progress of this project was as per plan. Readings from solar panel were first taken to find the possible input values of the converter. These values were then used as the manipulated variable in both the simulation and experimentation phase of the converter.

Simulation of the converter was done based on the overall block diagram of the circuit which gave positive outputs. The outputs of the simulation have achieved the targeted values. A few parameters of the simulated converter were observed such as the rise time, voltage ripple and the percentage error. From these observations, it was concluded that the simulated converter is accurate and reliable.

The circuit was later constructed to be tested. Multiple testing were done on the circuit to observe the output. The equipment used were multimeter and oscilloscope. The data from the observation was gathered and tabulated as well analysed. From the outcome, it can be seen that the physical circuit, identical to the simulation one, have been able to achieve its targeted outcome. All the output voltages are stable with variations of input voltage. Further analysis was done to find the percentage error of the circuit, which indicated that the converter's outputs have percentage error of a maximum value of 6.7%.

From all the analysis done, it can be seen that the circuit is accurate, reliable and robust. The project was able to achieve its objectives which are to study and investigate solar PV model for SIMO converter, to design a converter circuit to boost operations for electric vehicle applications and to simulate the circuit and analyse the functional output, justifying the results verified through working model. The proposed converter is suitable to be implemented and will be able to overcome the downsides of the conventional method of DC-DC converter used in electric vehicle. The researcher hopes that, with solving all these downsides, the research will benefit many people.

5.2 Recommendations

It is recommended that this converter's output voltage options are increased. This increase of voltage option, would correspond to the changes of the topology of the converter. Further analysis would need to be done on the constructed converter. As the electric vehicle development increases, future projects should get more feedback from the automotive industry about the latest technology and components available and modify the converter according to the requirement.

REFERENCES

[1] J. Hui, A. Bakhshai, and P. K. Jain, "A hybrid wind-solar energy system: A new rectifier stage topology," in *Applied Power Electronics Conference and Exposition (APEC), 2010 Twenty-Fifth Annual IEEE*, 2010, pp. 155-161.

[2] A. Emadi, Y. J. Lee, and K. Rajashekara, "Power Electronics and Motor Drives in Electric, Hybrid Electric, and Plug-In Hybrid Electric Vehicles," *IEEE Transactions on Industrial Electronics*, vol. 55, pp. 2237-2245, 2008.

[3] Kawahashi, "A new-generation hybrid electric vehicle and its supporting power semiconductor devices," in *Power Semiconductor Devices and ICs, 2004. Proceedings. ISPSD '04. The 16th International Symposium on*, 2004, pp. 23-29.

[4] T. Ahmed, T. K. Kha, S. M. Hasanuzzaman, T. Islam, A. Islam, A. Hoque, *et al.*, "Implementation of multi-input dual-output DC-DC boost converter using renewable energy for hybrid electric vehicle," in *Electrical Information and Communication Technology (EICT), 2015 2nd International Conference on*, 2015, pp. 223-227.

[5] A. Emadi, S. S. Williamson, and A. Khaligh, "Power electronics intensive solutions for advanced electric, hybrid electric, and fuel cell vehicular power systems," *IEEE Transactions on Power Electronics,* vol. 21, pp. 567-577, 2006.

[6] A. Nami, F. Zare, A. Ghosh, and F. Blaabjerg, "Multi-output DC-DC converters based on diode-clamped converters configuration: topology and control strategy," *IET Power Electronics,* vol. 3, pp. 197-208, 2010.

[7] E. Babaei, O. Abbasi, and S. Sakhavati, "An overview of different topologies of multi-port dc/dc converters for dc renewable energy source applications," in *2016 13th International Conference on Electrical*

Engineering/Electronics, Computer, Telecommunications and Information Technology (ECTI-CON), 2016, pp. 1-6.

[8] M. B. F. Prieto, S. P. Litran, E. D. Aranda, and J. M. E. Gomez, "New Single-Input, Multiple-Output Converter Topologies: Combining Single-Switch Nonisolated dc-dc Converters for Single-Input, Multiple-Output Applications," *IEEE Industrial Electronics Magazine,* vol. 10, pp. 6-20, 2016.

[9] R. Hou, P. Magne, B. Bilgin, and A. Emadi, "A topological evaluation of isolated DC/DC converters for Auxiliary Power Modules in Electrified Vehicle applications," in *2015 IEEE Applied Power Electronics Conference and Exposition (APEC)*, 2015, pp. 1360-1366.

[10] Texas Instruments, “Basic Calculation of a Boost Converter’s Power Stage” SLVA372C datasheet, Nov. 2009 [Revised Jan. 2014].

[11] XLSEMI, “400KHz 42V 5A Switching Current Boost DC/DC Converter” XL6009 datasheet.

[12] Texas Instruments, “Understanding Boost Power Stages in Switchmode Power Supply” SLVA061 datasheet, Mar. 1999.1